

**Ejecta-CSM interaction model
for low-luminosity GRBs:
application to IIGRB 171205A**

Akihiro Suzuki (NAOJ)

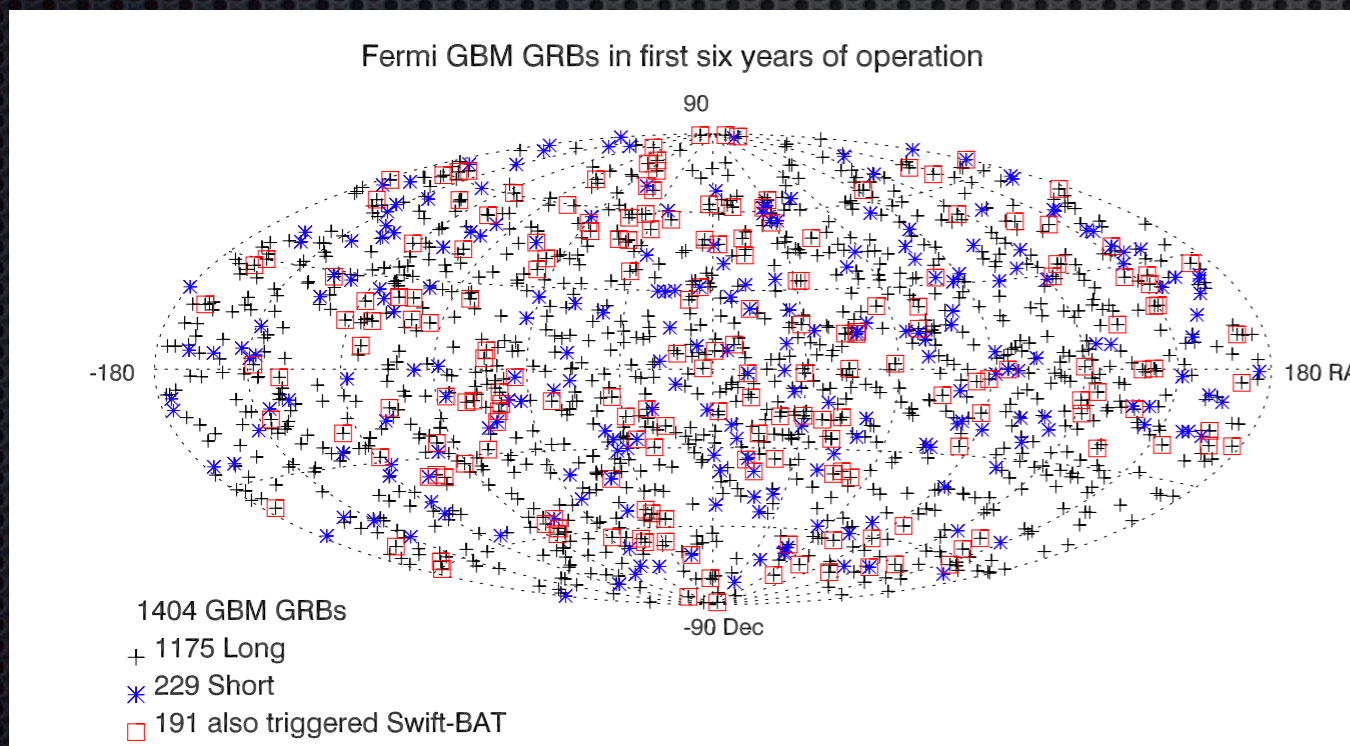
Suzuki, Maeda, & Shigeyama (2017), ApJ, 832,32

Suzuki, Maeda, & Shigeyama (2018), in prep

- Introduction
- Ejecta-CSM interaction
- Light curve fitting for GRB171205A
- Conclusion

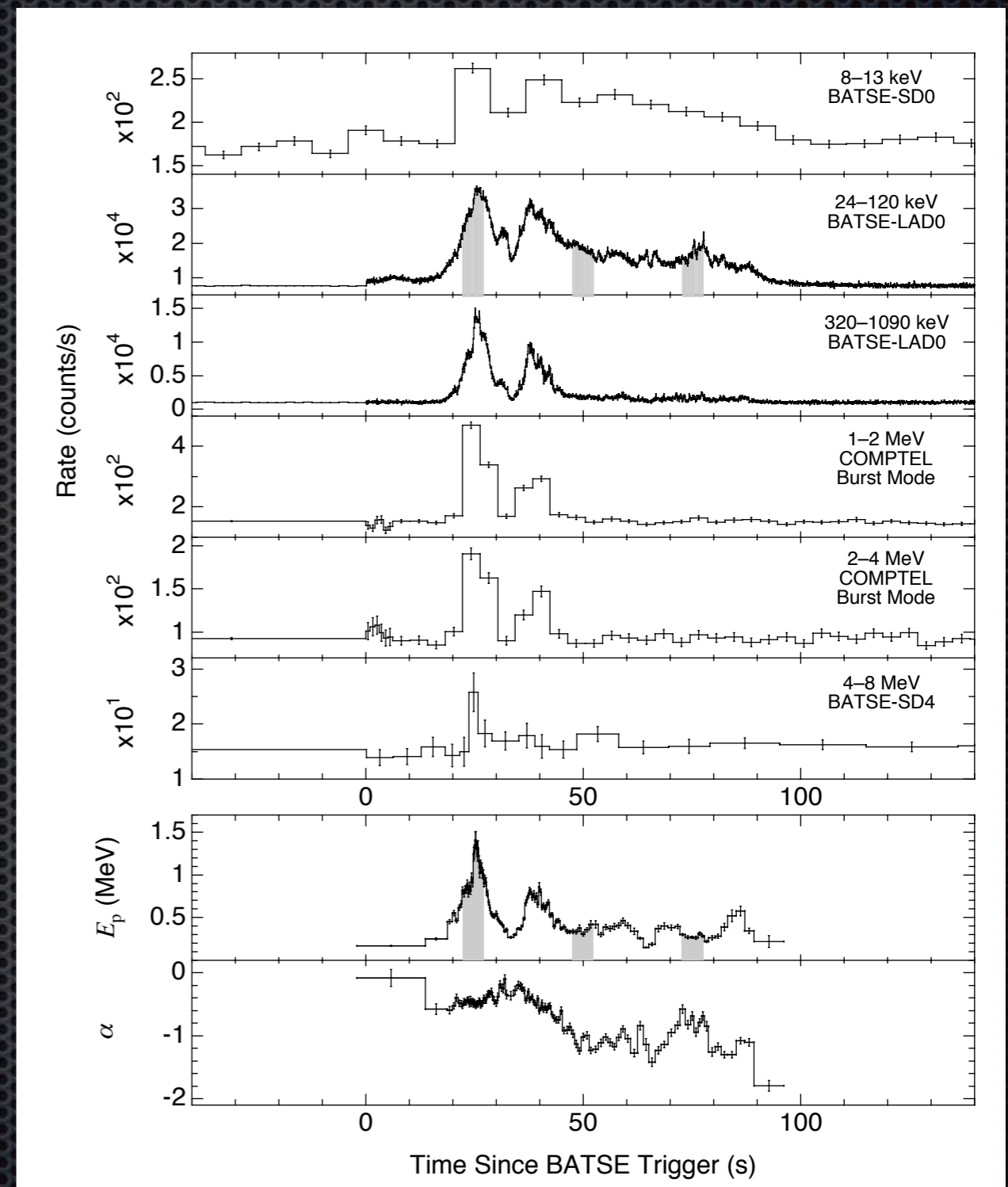
Gamma-ray bursts

- bursts of gamma-ray photons: ~ 1 event/day, isotropic
- spectrum well represented by a "Band function" (Band et al. 1993)
- classification: long-soft/short-hard



distribution of Fermi GRBs on the celestial sphere

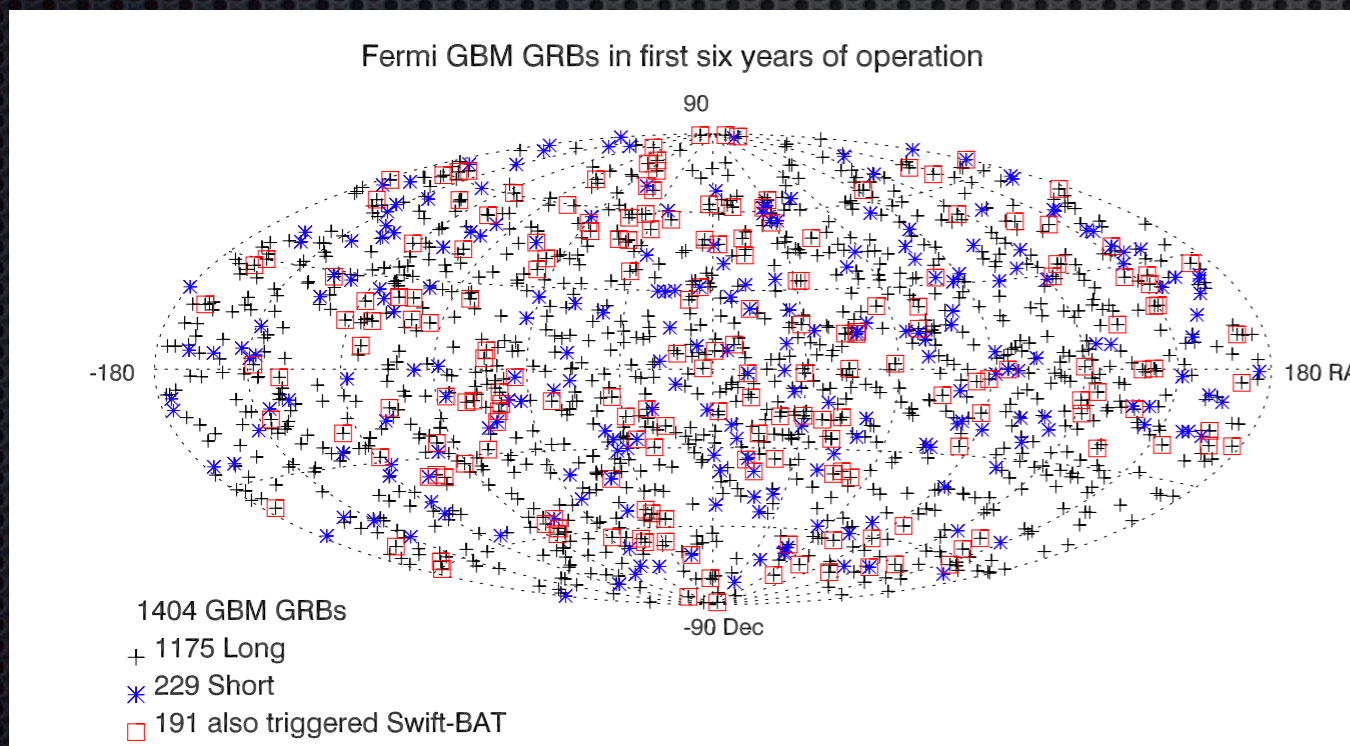
(3rd Fermi GBM catalog, 2016)



Briggs+ (1999)

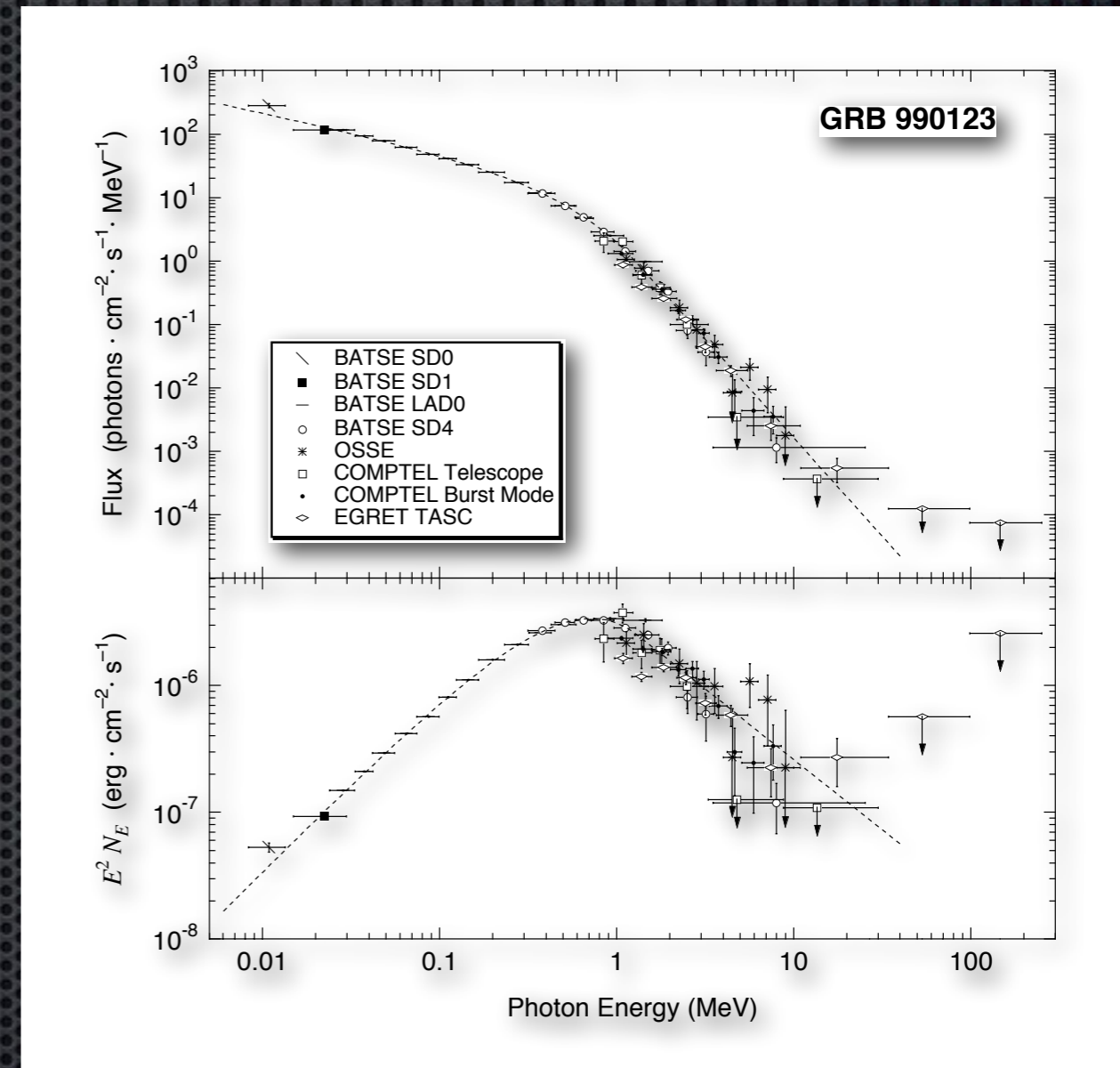
Gamma-ray bursts

- bursts of gamma-ray photons: ~1 event/day, isotropic
- spectrum well represented by a "Band function" (Band et al. 1993)
- classification: long-soft/short-hard



distribution of Fermi GRBs on the celestial sphere

(3rd Fermi GBM catalog, 2016)

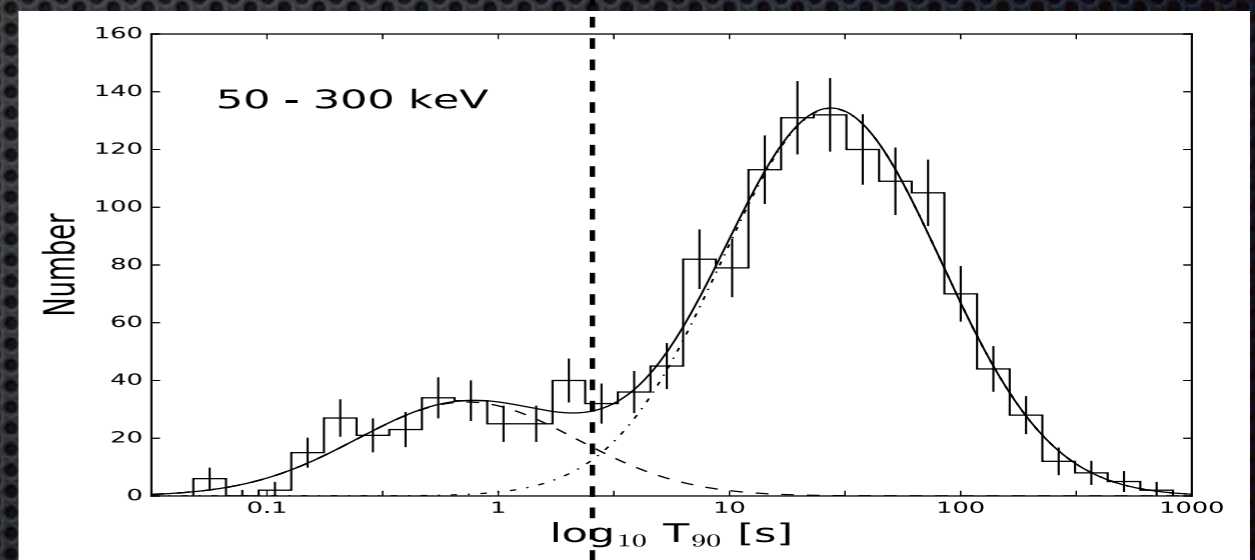
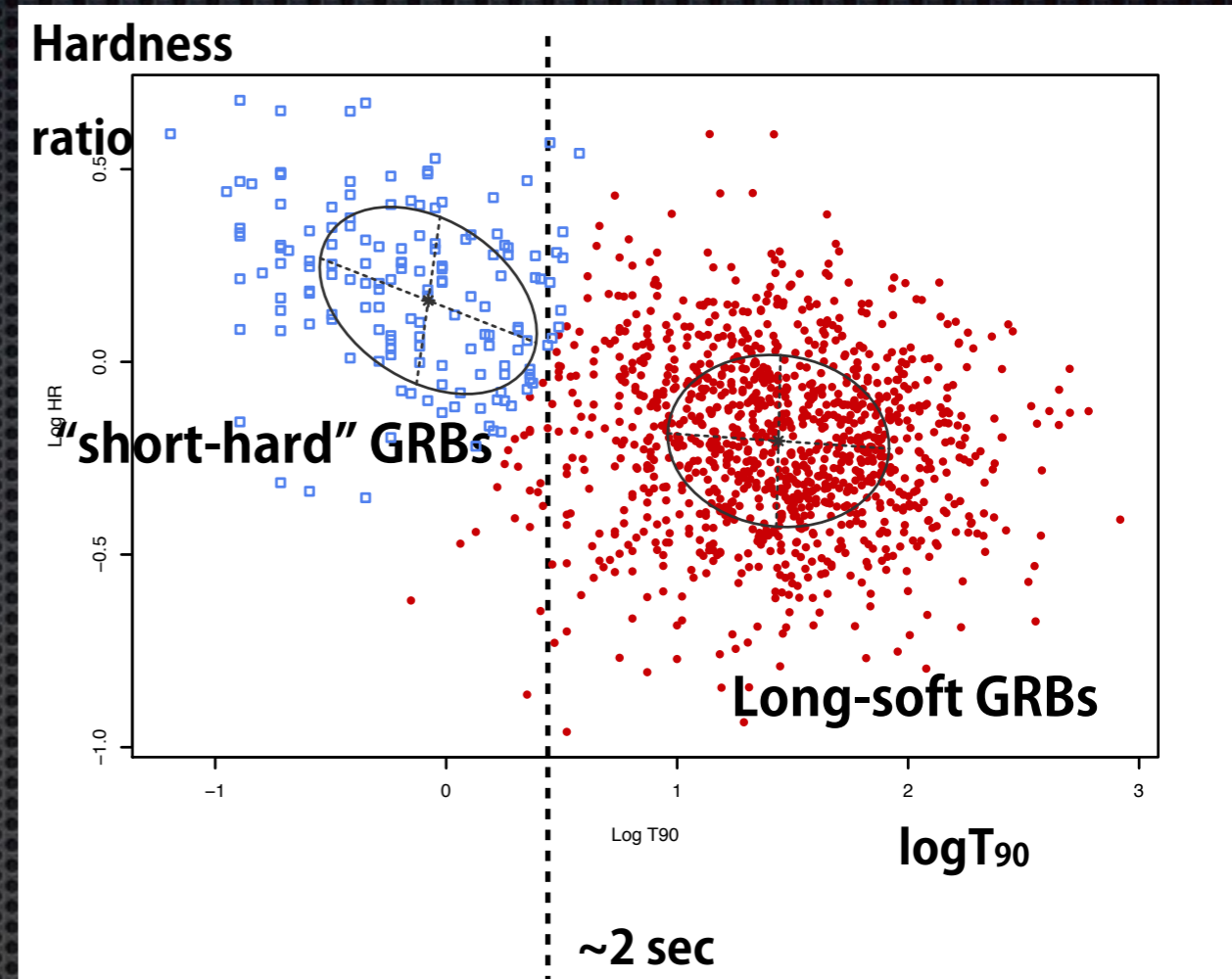


Briggs+ (1999)

Gamma-ray bursts

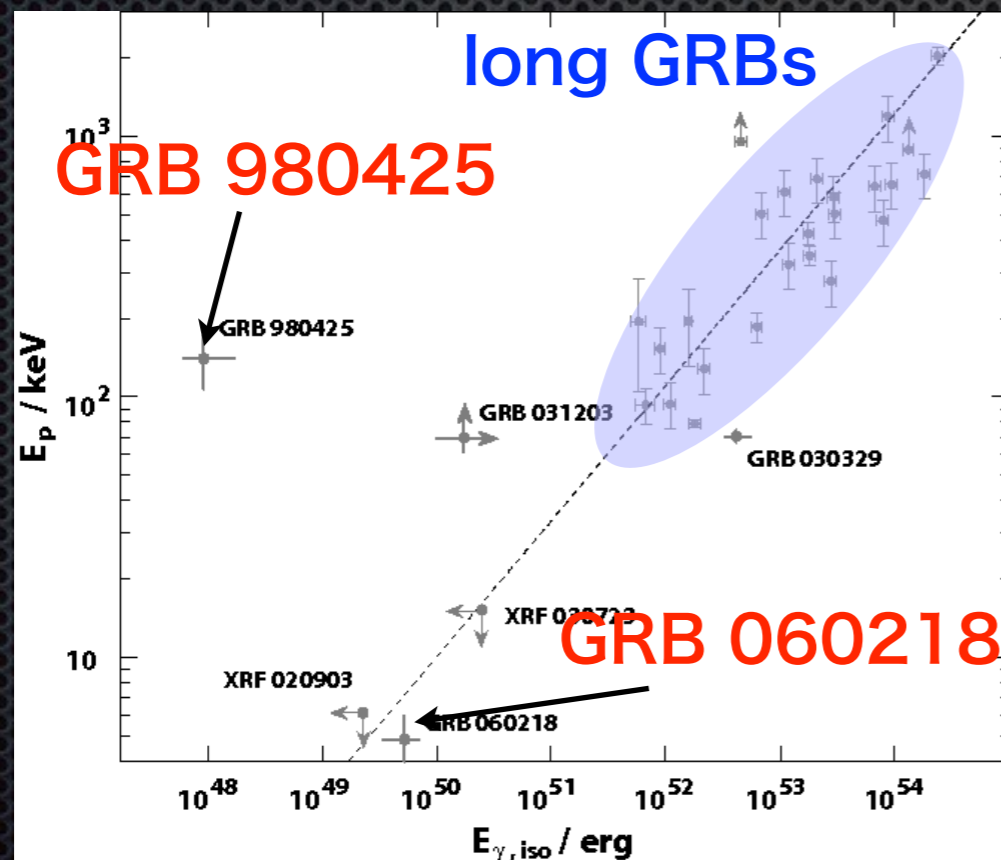
- bursts of gamma-ray photons: ~ 1 event/day, isotropic
- spectrum well represented by a "Band function" (Band et al. 1993)
- classification: long-soft/short-hard

HR vs T90 plot(3rd Fermi GBM catalog, 2016)

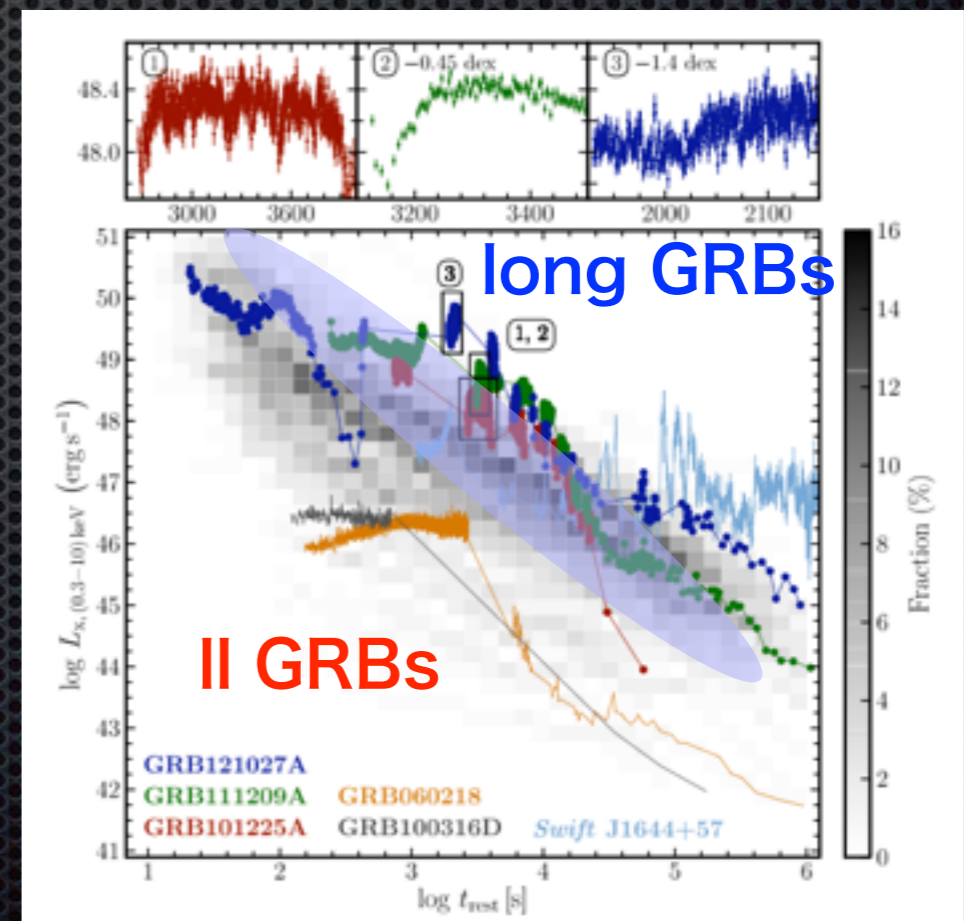


low-luminosity GRBs

- ➔ sub-energetic class of long GRBs
- ➔ only nearby events are detected, but event rate is high
e.g., $230^{+490}_{-190} \text{ Gpc}^{-3} \text{ yr}^{-1}$ (Soderberg+ 2006), $100\text{-}1800 \text{ Gpc}^{-3} \text{ yr}^{-1}$ (Guetta&Della Valle 2007)
- ➔ They accompany broad-lined Ic SNe
- ➔ Ex. GRB 980425/SN 1998bw, GRB 060218/SN 2006aj, GRB100316D/ SN2010bh



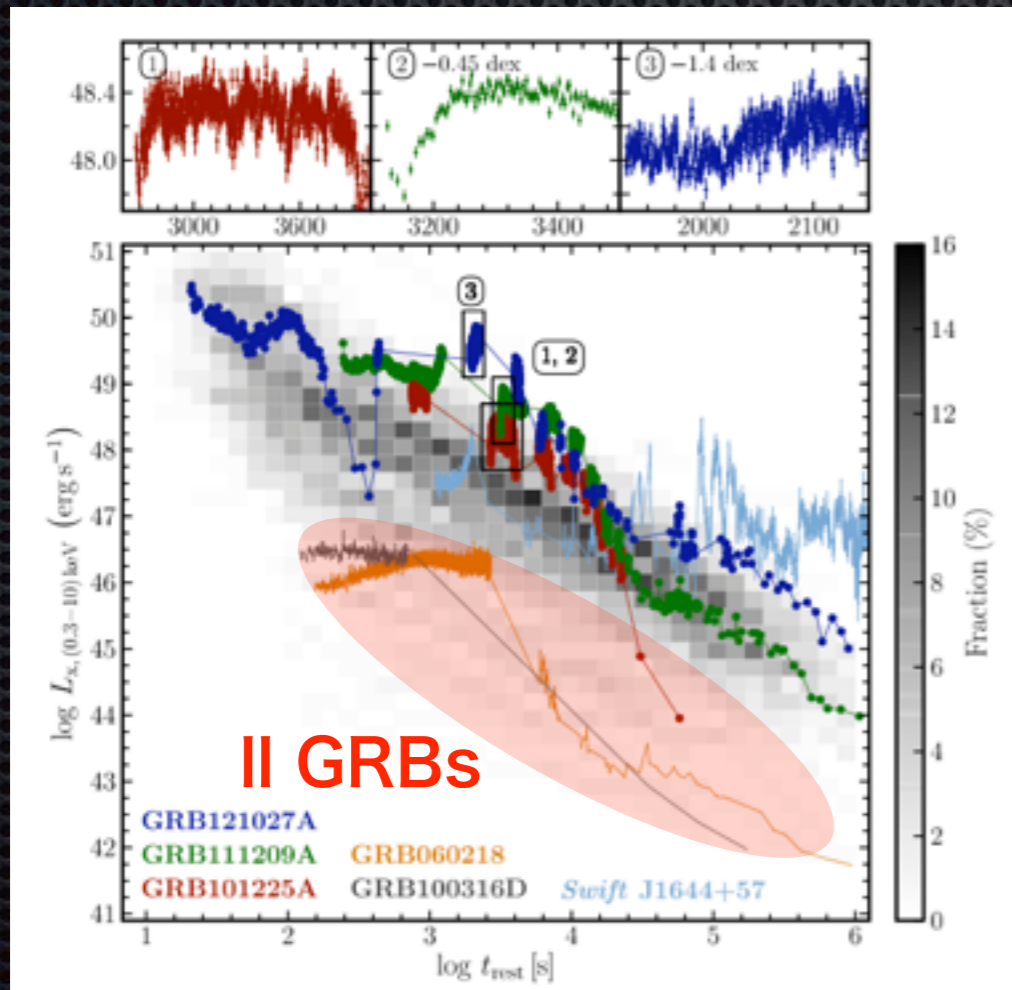
Kaneko+ (2006)



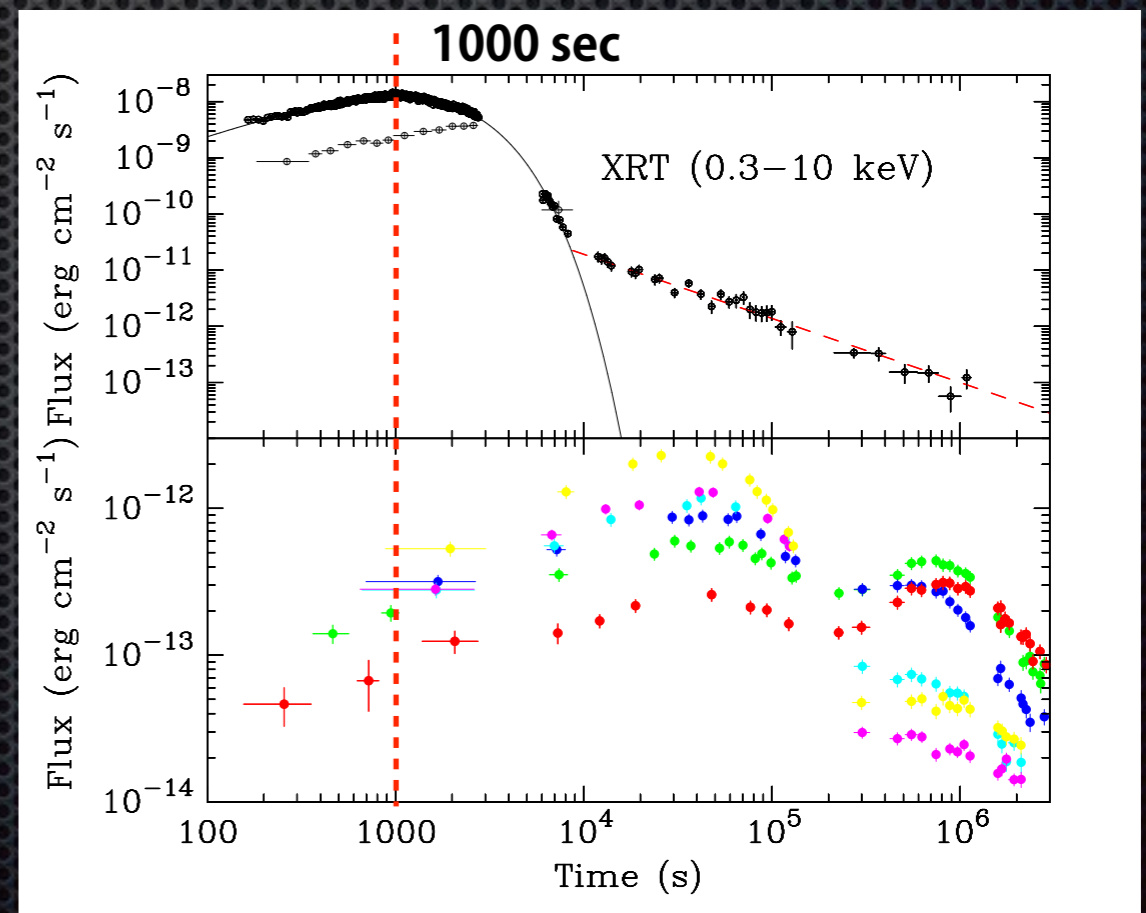
Levan+ (2013)

low-luminosity GRBs

- ➔ sub-energetic class of long GRBs
- ➔ only nearby events are detected, but event rate is high
e.g., 230^{+490}_{-190} Gpc⁻³ yr⁻¹ (Soderberg+ 2006), 100-1800 Gpc⁻³ yr⁻¹ (Guetta&Della Valle 2007)
- ➔ They accompany broad-lined Ic SNe
- ➔ Ex. GRB 980425/SN 1998bw, GRB 060218/SN 2006aj, GRB100316D/ SN2010bh



Levan+(2013)



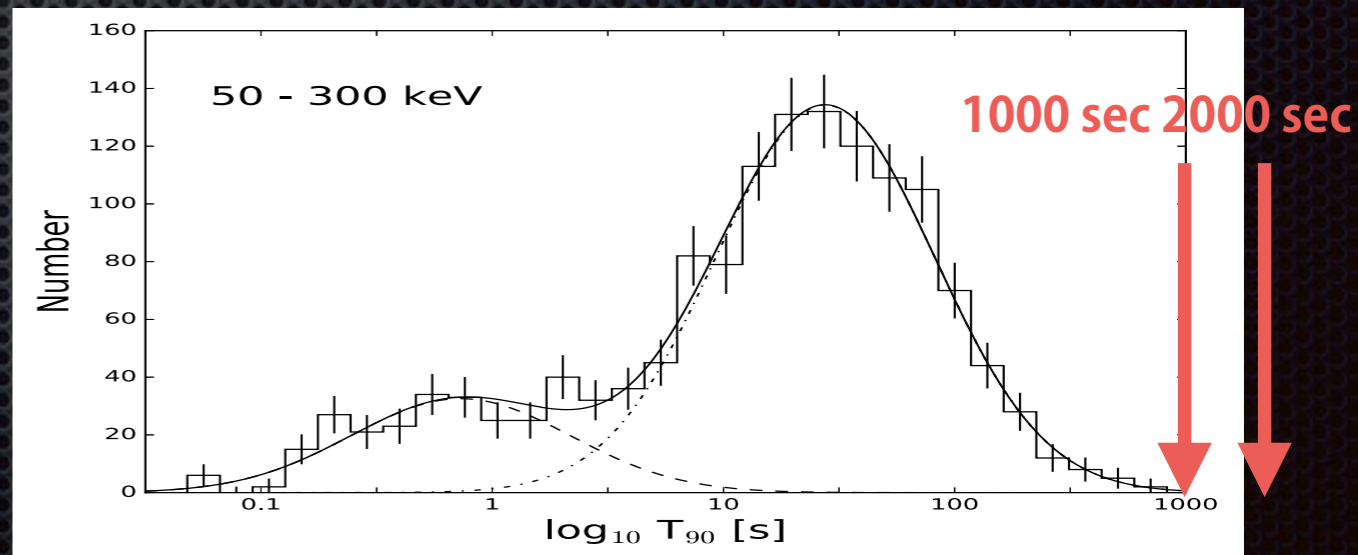
GRB 060218, Campana+ (2006)

low-luminosity GRBs

- GRB 980425/SN 1998bw, GRB 060218/SN 2006aj, GRB 100316D/SN 2010bh
- low L_{iso} , low E_{peak}

	Luminosity $L_{\gamma,iso}$	Isotropic energy E_{iso}	Duration T_{90}	peak energy E_p
GRB 980425 SN 1998bw	6×10^{46} erg/s	9×10^{47} erg	35 s	122 keV
GRB 060218 SN 2006aj	2×10^{46} erg/s	4×10^{49} erg	2100 s	4.7 keV
GRB 100316D SN 2010bh	5×10^{46} erg/s	6×10^{49} erg	1300 s	18 keV

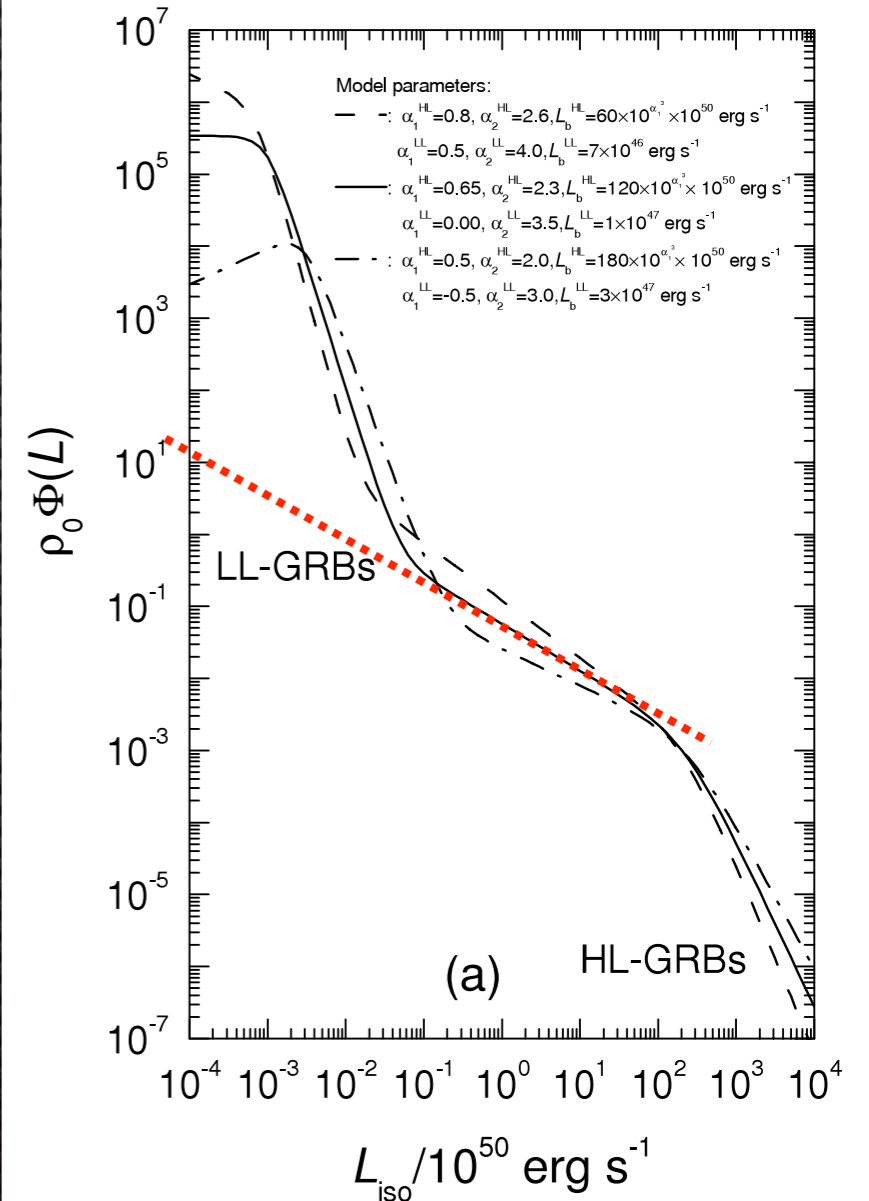
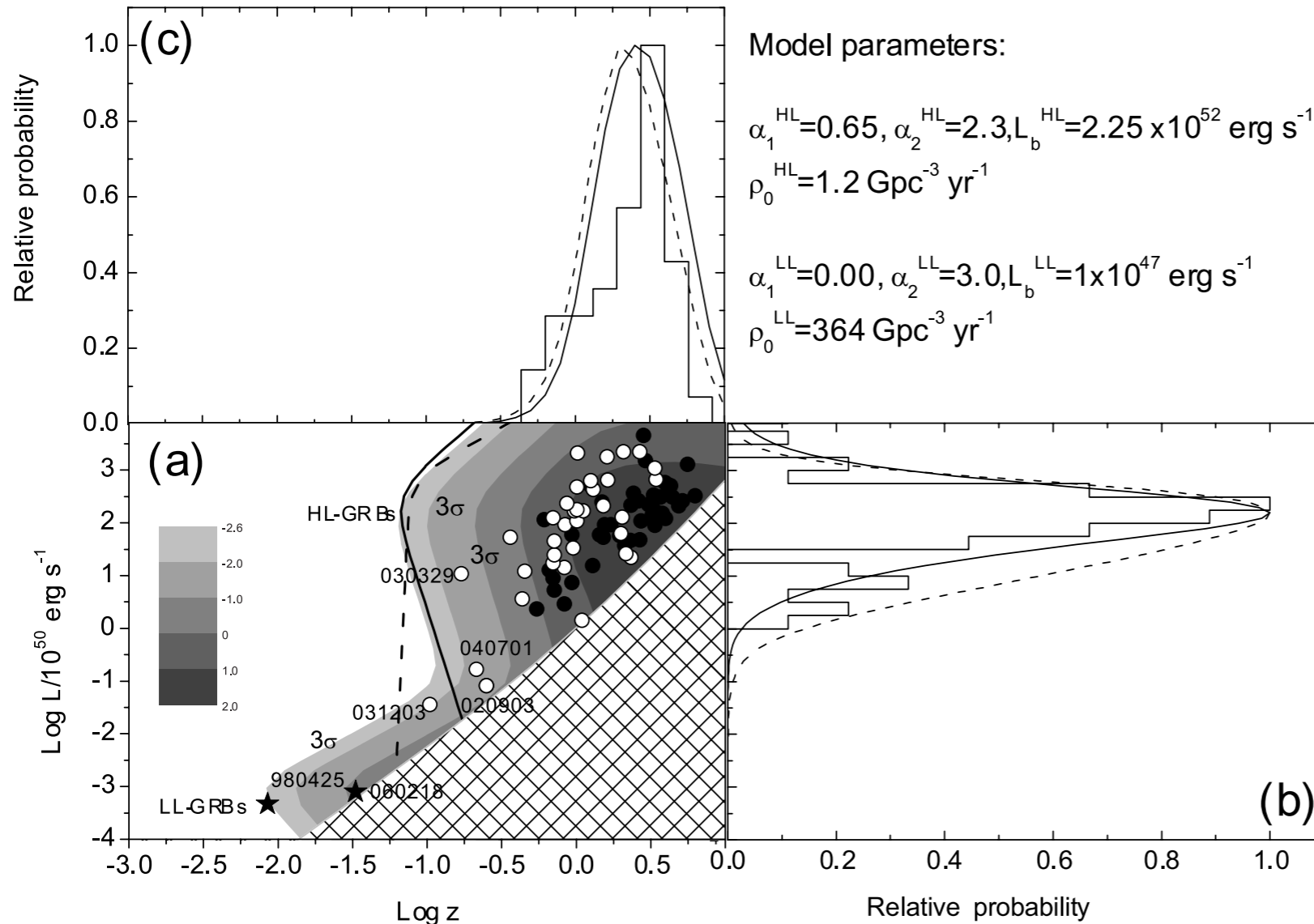
cf. $L_{iso} \sim 10^{51}$ erg/s, $E_{iso} \sim 10^{52-53}$ erg for standard GRBs



low-luminosity GRBs

- ➔ GRB 980425/SN 1998bw, GRB 060218/SN 2006aj, GRB 100316D/SN 2010bh
- ➔ low L_{iso} , low E_{peak}
- ➔ luminosity function

Liang+ (2007)

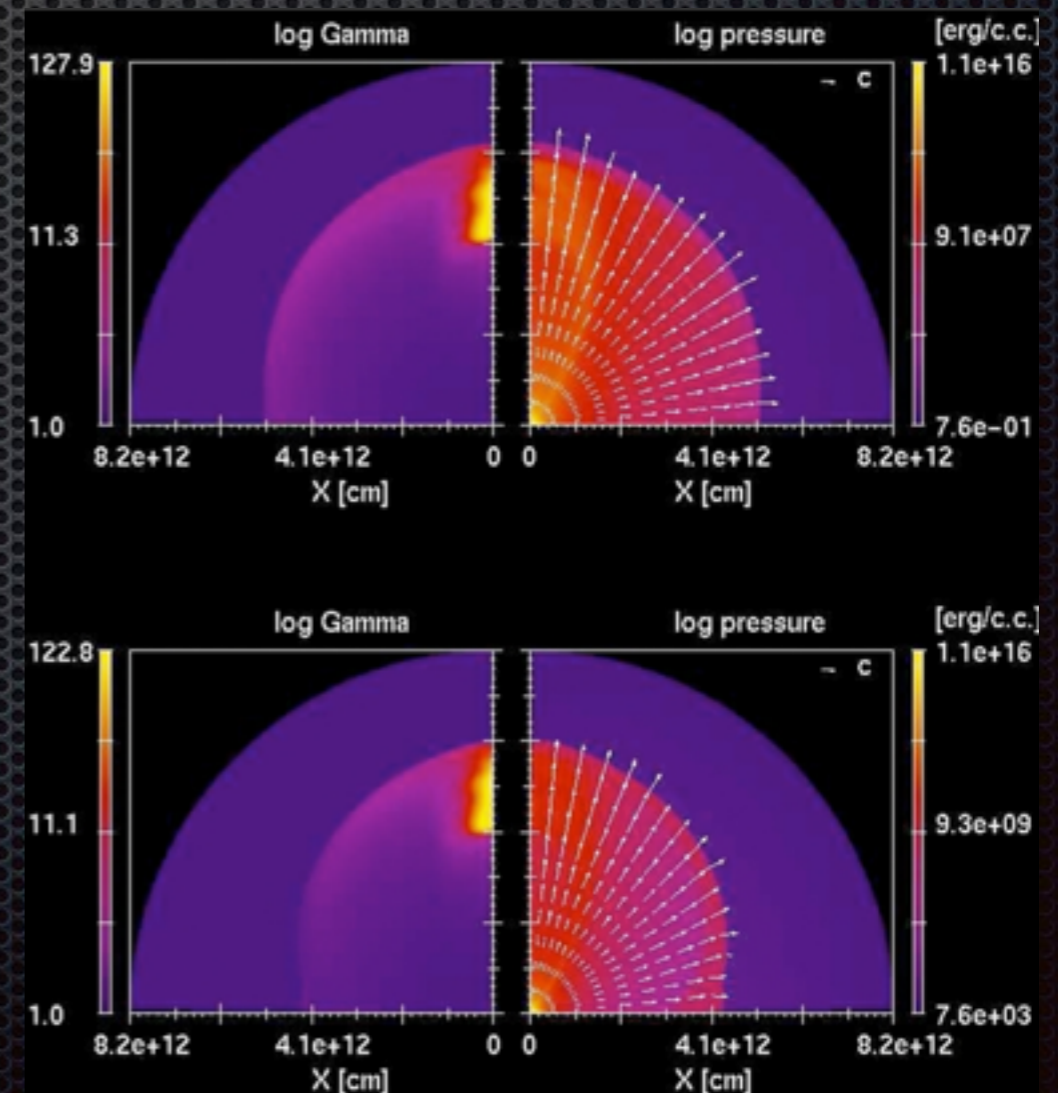
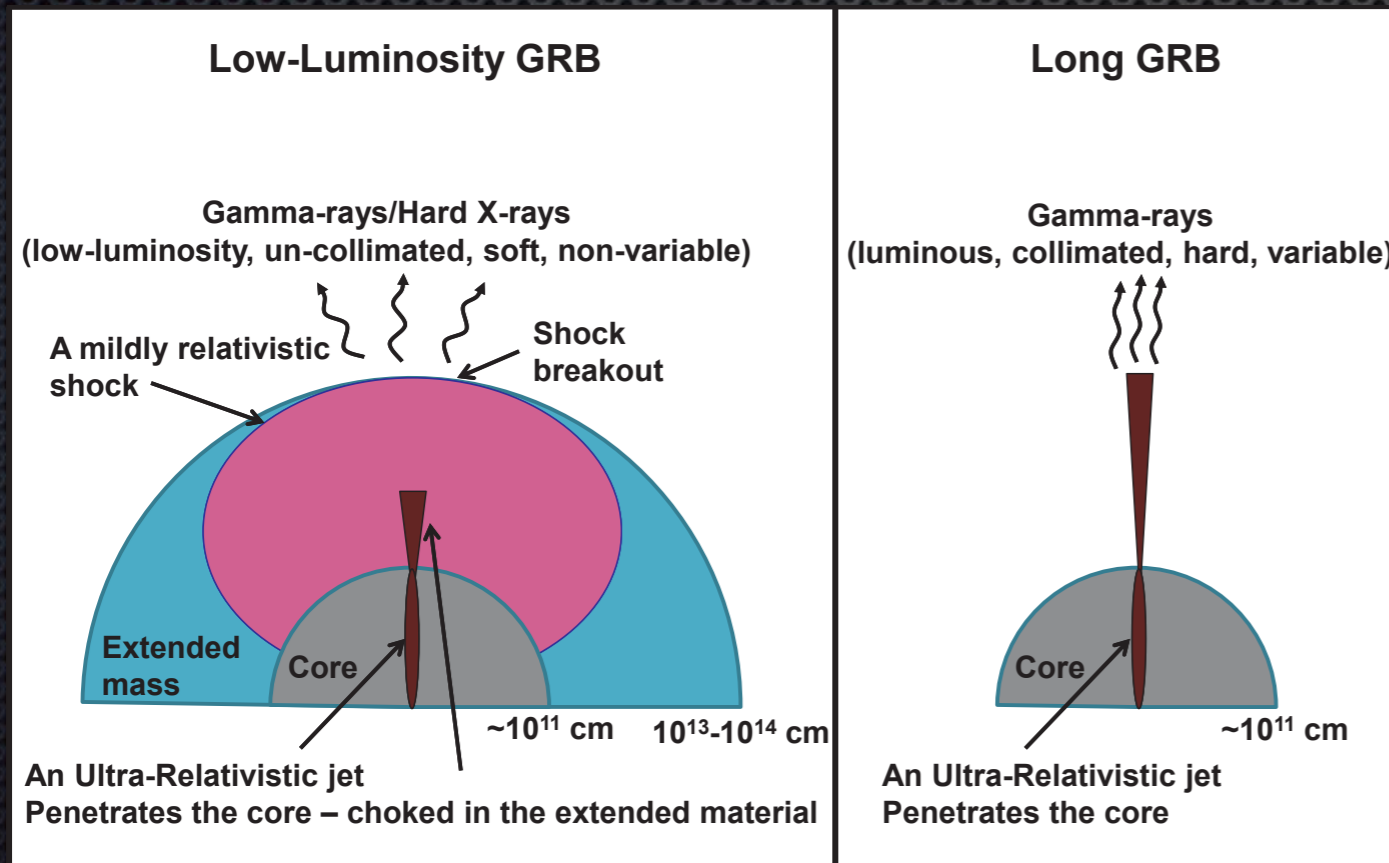


Origin of low-luminosity GRBs

- central engine was a neutron star? (e.g., Mazzali+2006)
- relativistic shock breakout with dense CSM, off-axis/weak/failed jet, cocoon-CSM interaction (Kulkarni+1998, Tan+2001, Campana+2006, Li 2007; Toma+2007; Wang+ 2007; Waxman+ 2007, Suzuki&Shigeyama 2012, Nakar 2015, Irwin&Chevalier 2016)

Suzuki&Shigeyama (2013)

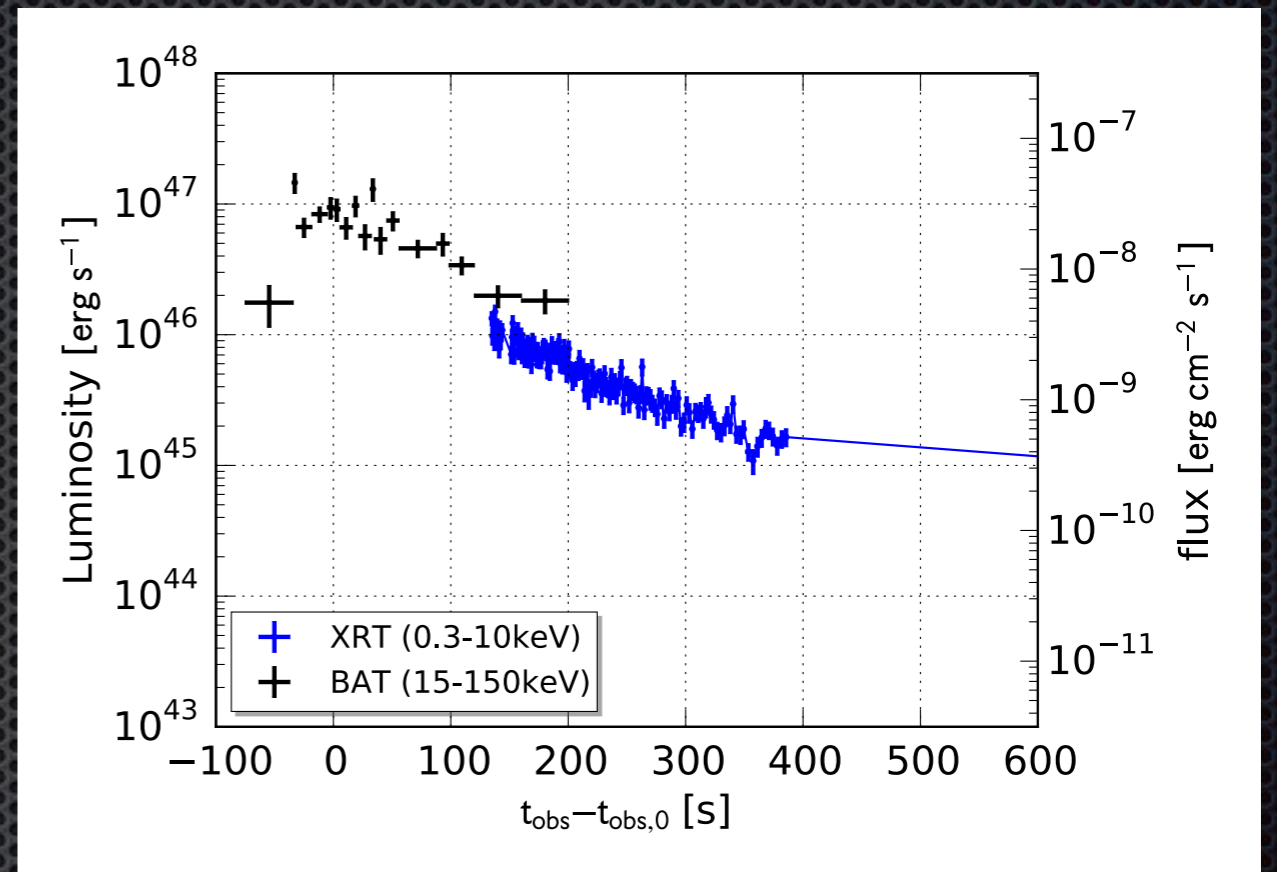
Nakar (2015)



New LLGRB 171205A @ 168Mpc

- ➔ Swift detection on 2017/12/05
(D'Elia+2017, GCN circular 22177)
- ➔ $E_{\text{iso}} \sim 1.2 \times 10^{49}$ [erg], $T_{90} \sim 190$ [s]
(Lien+2017, GCN circular 22184)
- ➔ follow-up optical, radio observation
- ➔ SN bump after a few days
(de Ugarte Postigo+2017, GCN circular 22207)

Obs. Data provided by Swift UK Data Centre



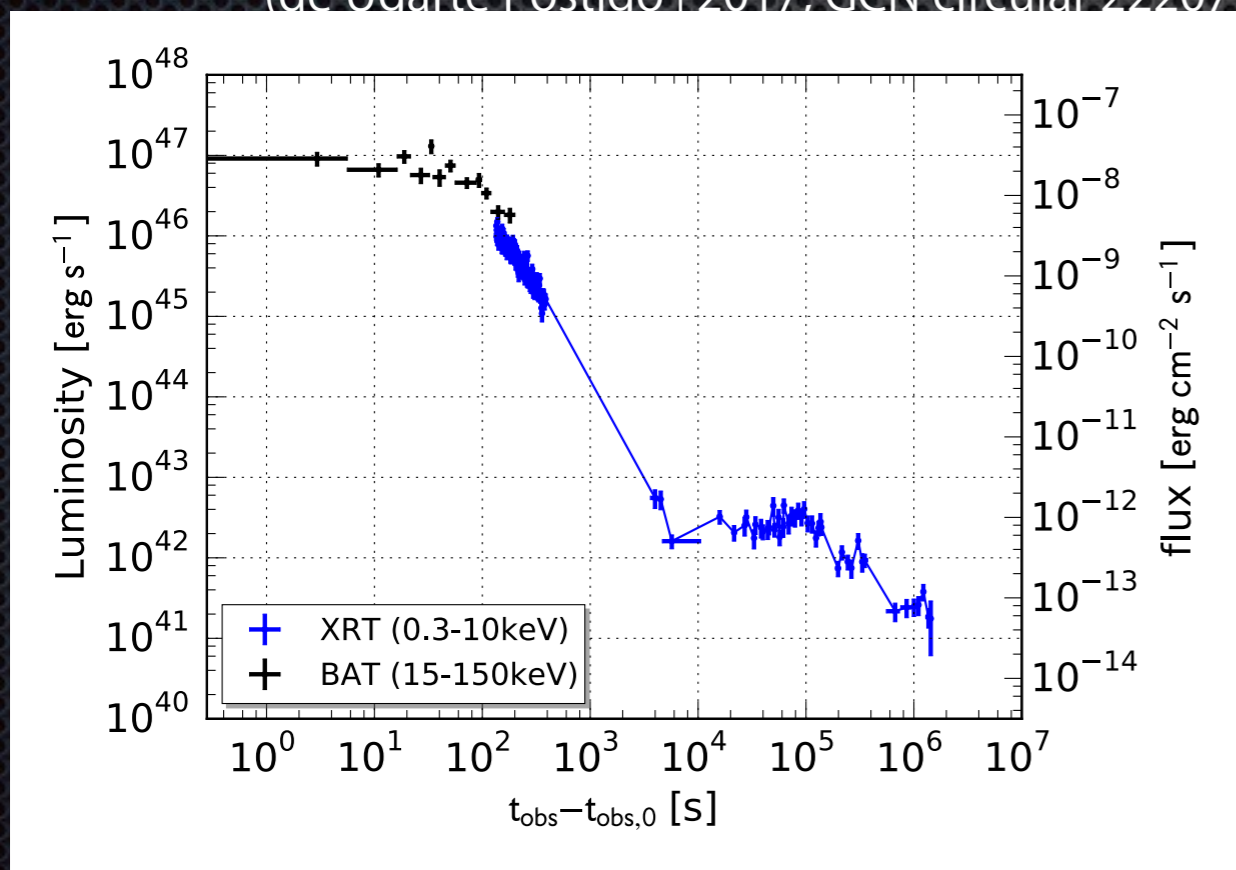
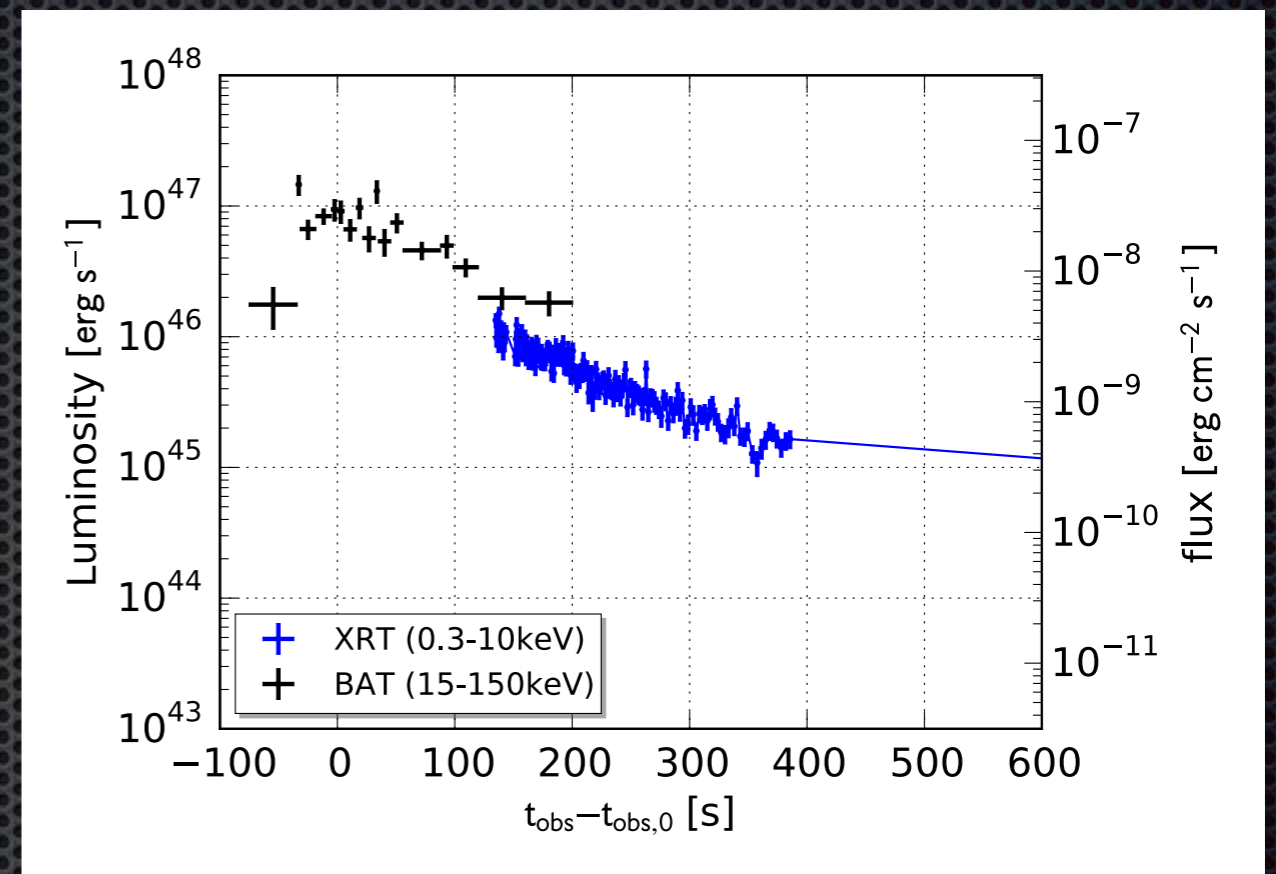
	Luminosity $L_{\gamma, \text{iso}}$	Isotropic energy E_{iso}	Duration T_{90}	peak energy E_p
GRB 980425 SN 1998bw	6×10^{46} erg/s	9×10^{47} erg	35 s	122 keV
GRB 060218 SN 2006aj	2×10^{46} erg/s	4×10^{49} erg	2100 s	4.7 keV
GRB 100316D SN 2010bh	5×10^{46} erg/s	6×10^{49} erg	1300 s	18 keV
GRB 171205A SN 2017iuk	6×10^{46} erg/s	1.2×10^{49} erg	190 s	N/A (single PL)

cf. $L_{\text{iso}} \sim 10^{51}$ erg/s, $E_{\text{iso}} \sim 10^{52-53}$ erg for standard GRBs

New LLGRB 171205A @ 168Mpc

- ➔ Swift detection on 2017/12/05
(D'Elia+2017, GCN circular 22177)
- ➔ $E_{iso} \sim 1.2 \times 10^{49}$ [erg], $T_{90} \sim 190$ [s]
(Lien+2017, GCN circular 22184)
- ➔ follow-up optical, radio observation
- ➔ SN bump after a few days
(de Ugarte Postigo+2017, GCN circular 22207)

Obs. Data provided by Swift UK Data Centre



isotropic energy E_{iso}	Duration T_{90}	peak energy E_p
10^{47} erg	35 s	122 keV
10^{49} erg	2100 s	4.7 keV
10^{49} erg	1300 s	18 keV
1.1×10^{49} erg	190 s	N/A (single PL)

SN 2017iuk

10^{47} erg/s

1.1×10^{49} erg

190 s

N/A (single PL)

cf. $L_{iso} \sim 10^{51}$ erg/s, $E_{iso} \sim 10^{52-53}$ erg for standard GRBs

- Introduction
- Ejecta-CSM interaction
- Light curve fitting for GRB171205A
- Conclusion

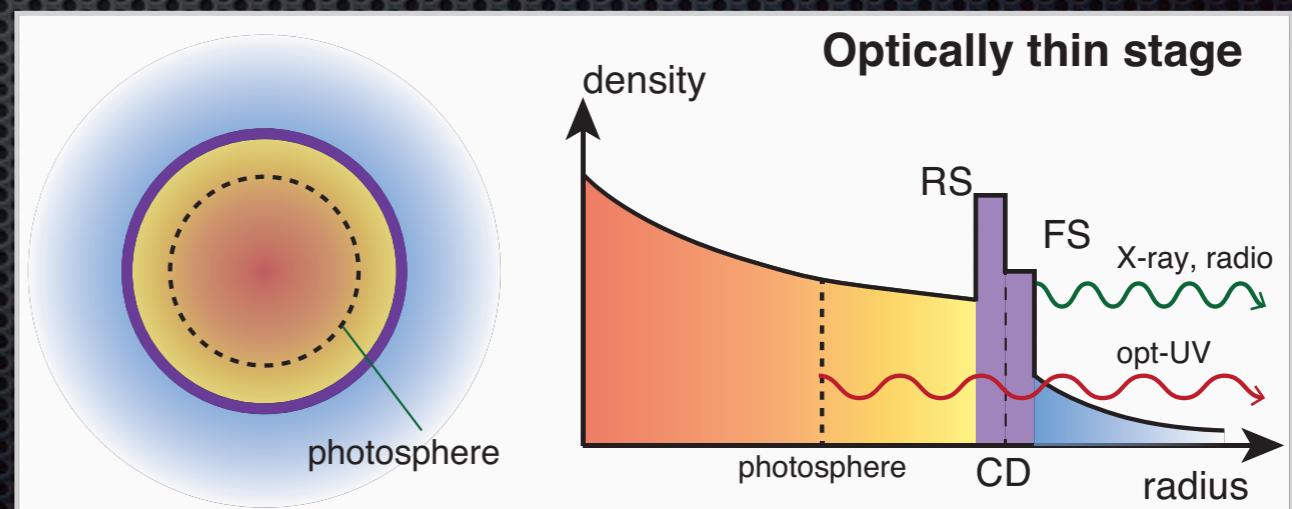
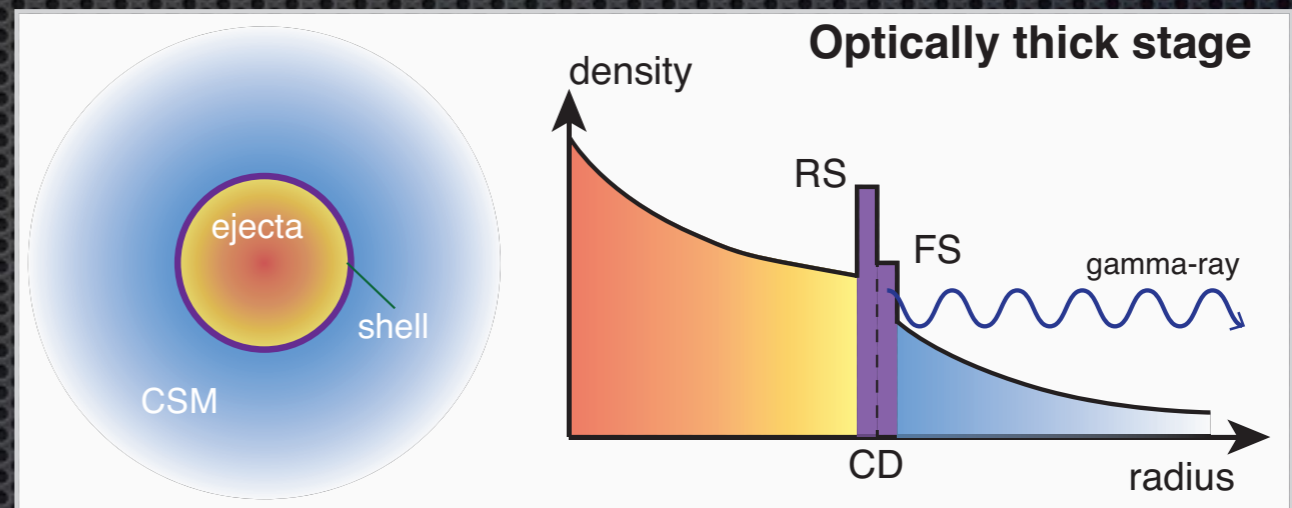
Ejecta with mildly relativistic speeds and CSM

- ➔ SN ejecta (with max $\Gamma \sim 2-10$) colliding with circum-stellar medium (CSM), leading to the dissipation of the kinetic energy into the thermal energy of the shocked gas.
- ➔ the thermal energy diffusing out through the shell is responsible for the prompt emission

How much energy can be released in ejecta-CSM interaction?

- kinetic energy of SN ejecta
- density structure
- CSM density

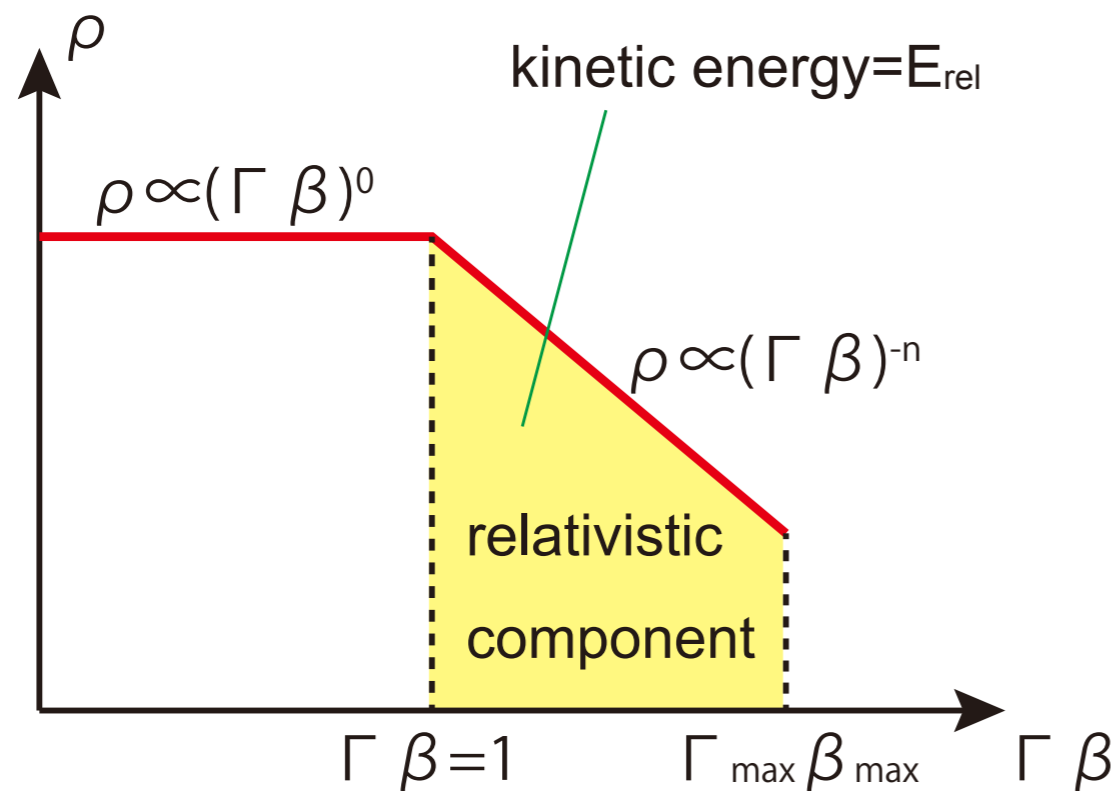
Suzuki, Maeda, Shigeyama (2018)



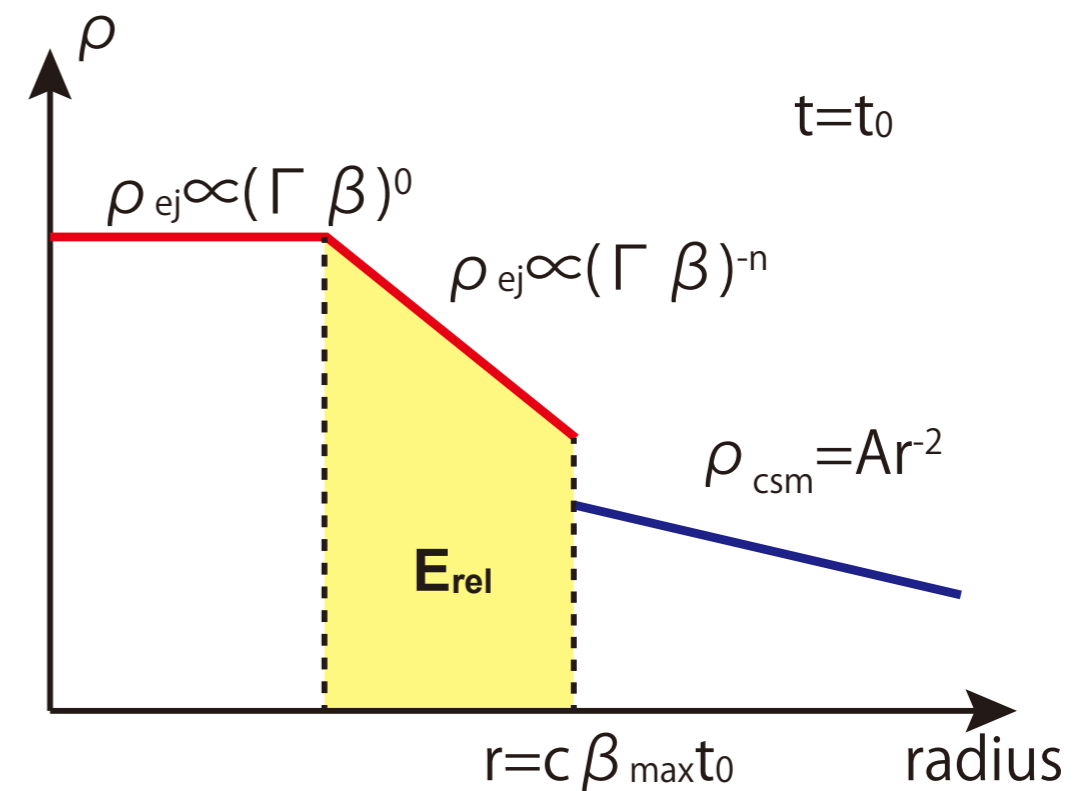
1D simulation with spherical symmetry

- steady wind: $\rho = Ar^{-2}$, $A_{\star} = A / (5 \times 10^{11} \text{ [g/cm]}) = 10$
 ($dM/dt = 10^{-4} M_{\odot}/\text{yr}$, for $v_{\text{wind}} = 1000 \text{ km/s}$)
- freely expanding trans-relativistic ejecta: $c\beta = r/t$,
 $\Gamma_{\text{max}} = 10$, $E_{\text{rel}} = 10^{51} \text{ [erg]}$, $t_0 = 10 \text{ [sec]}$, $n = 5$

Ejecta distribution in velocity space

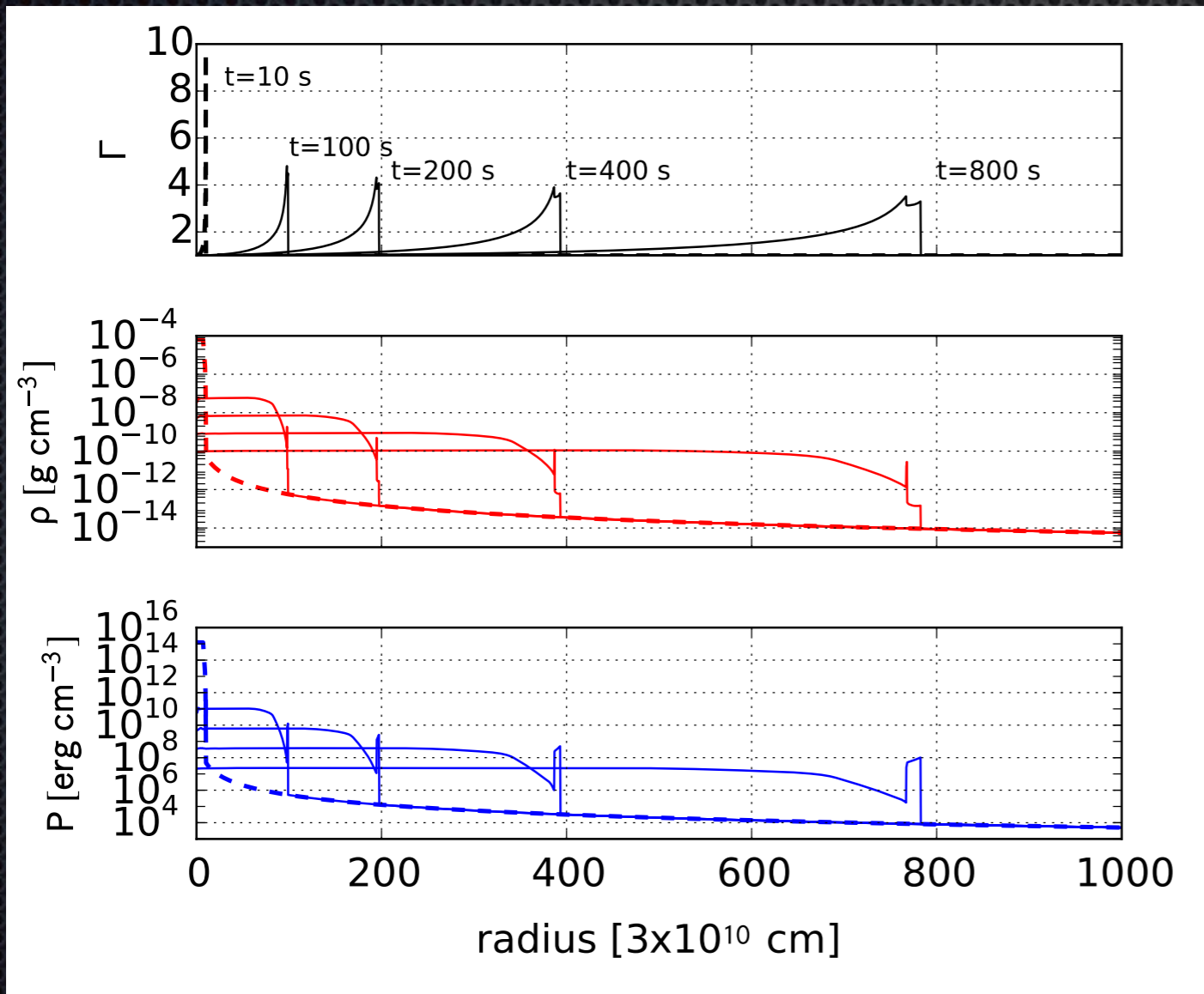


Ejecta distribution in physical space



1D simulation with spherical symmetry

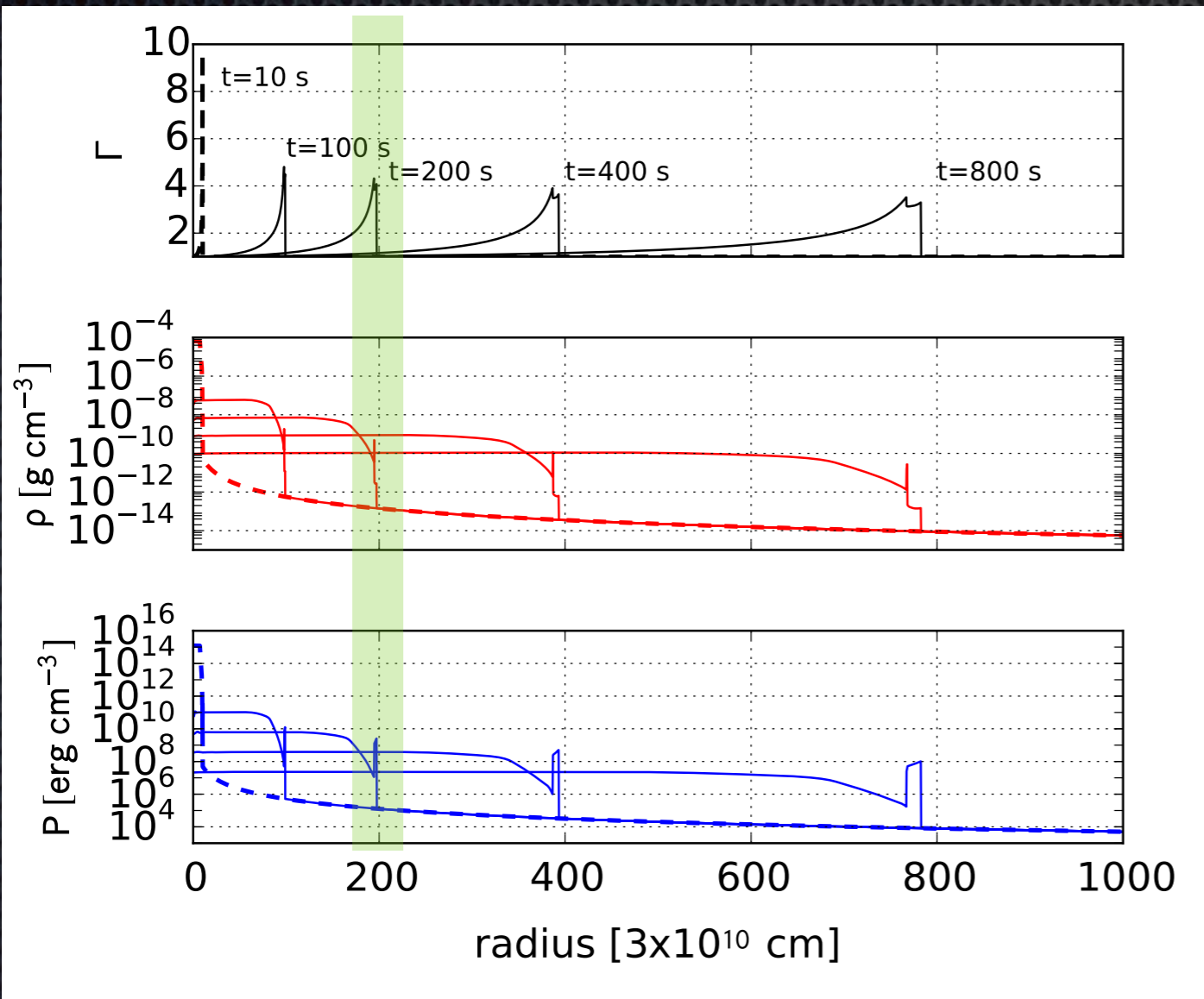
- ➔ forward/reverse shock formation by ejecta-CSM interaction.
- ➔ geometrically thin shell between the shocks is expanding into the outer region.



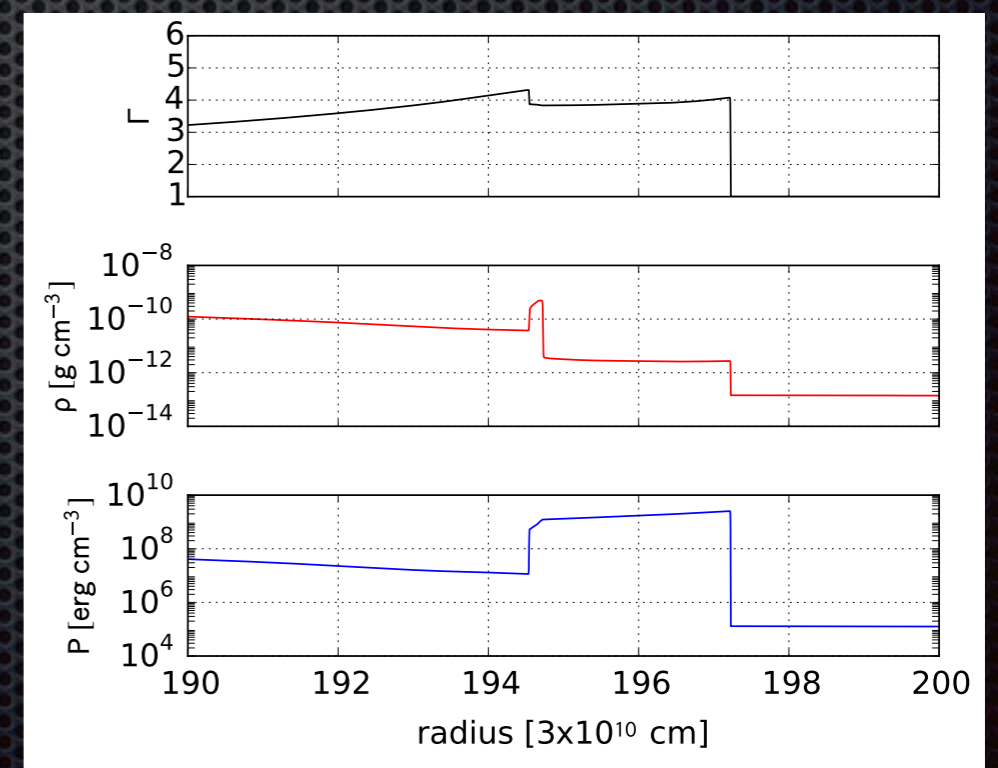
Suzuki, Maeda, Shigeyama (2017)

1D simulation with spherical symmetry

- ➔ forward/reverse shock formation by ejecta-CSM interaction.
- ➔ geometrically thin shell between the shocks is expanding into the outer region.

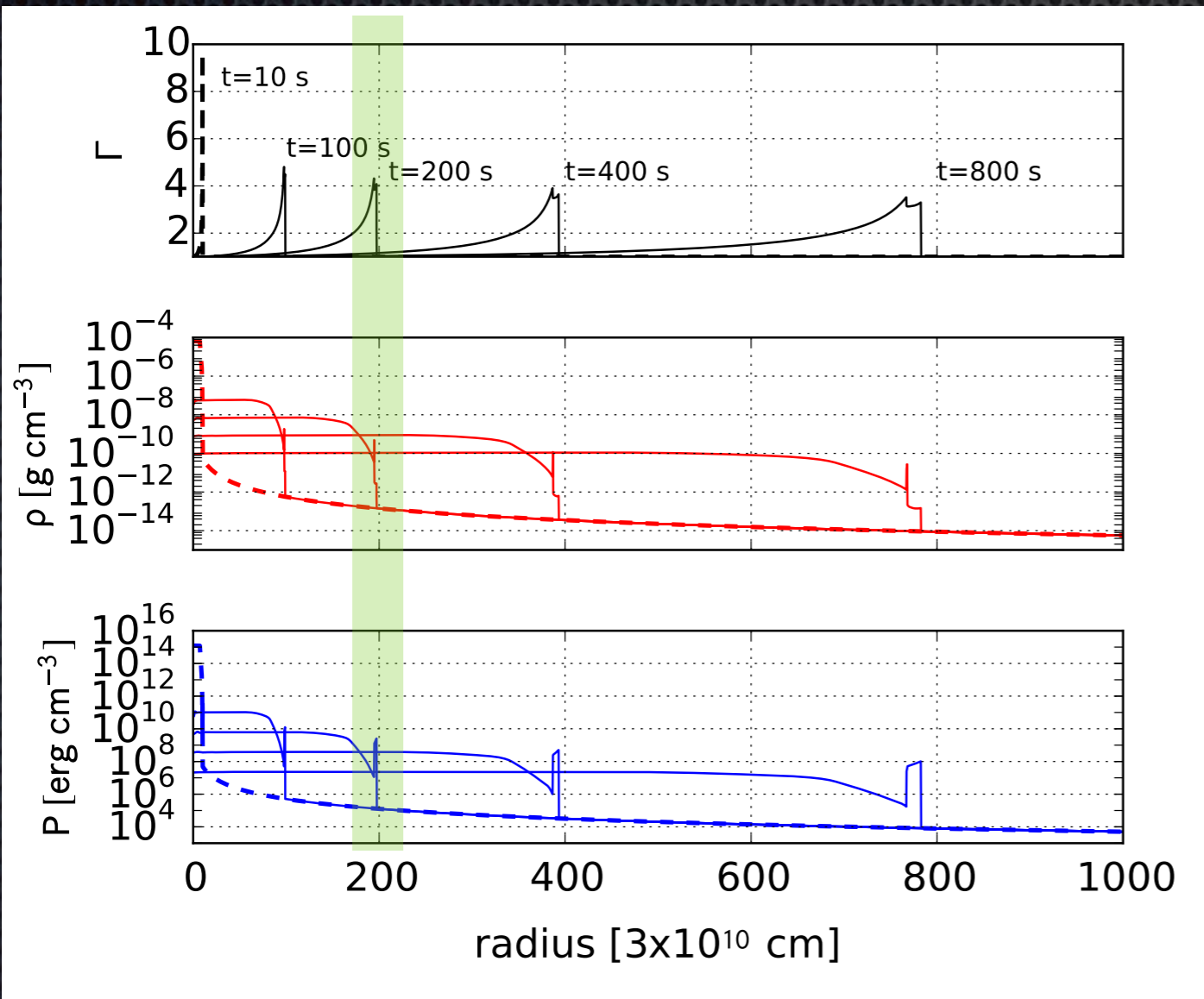


Suzuki, Maeda, Shigeyama (2017)

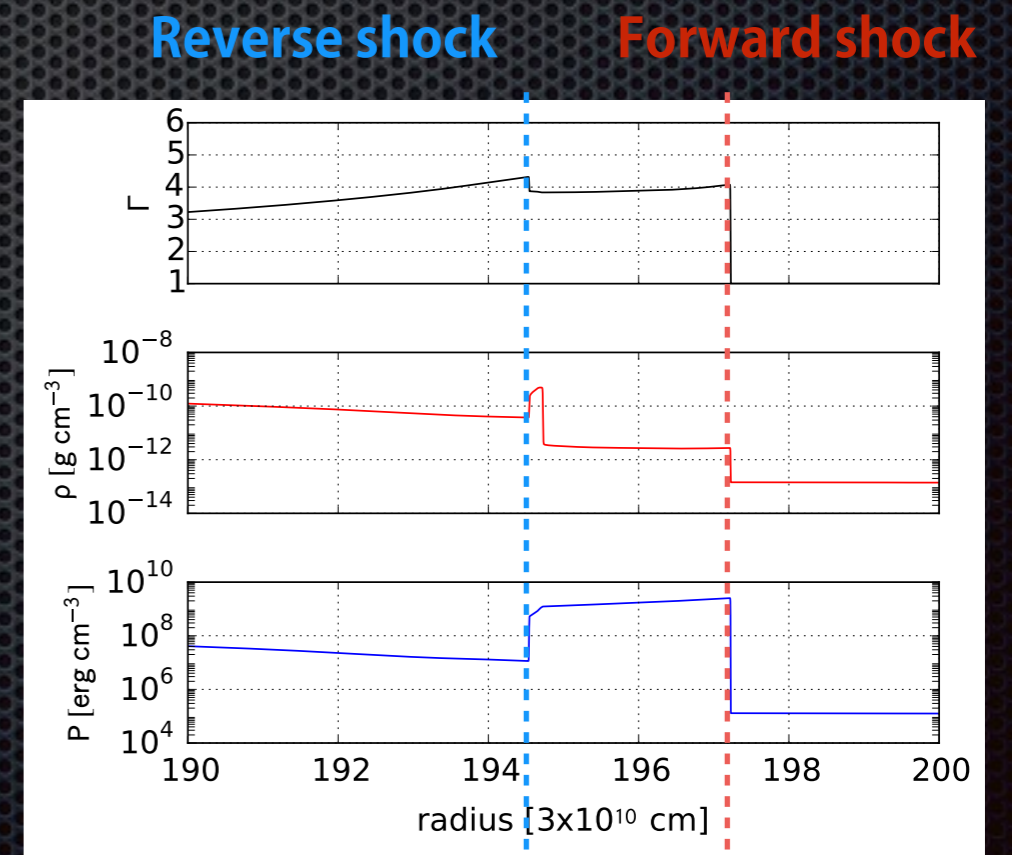


1D simulation with spherical symmetry

- ➔ forward/reverse shock formation by ejecta-CSM interaction.
- ➔ geometrically thin shell between the shocks is expanding into the outer region.



Suzuki, Maeda, Shigeyama (2017)

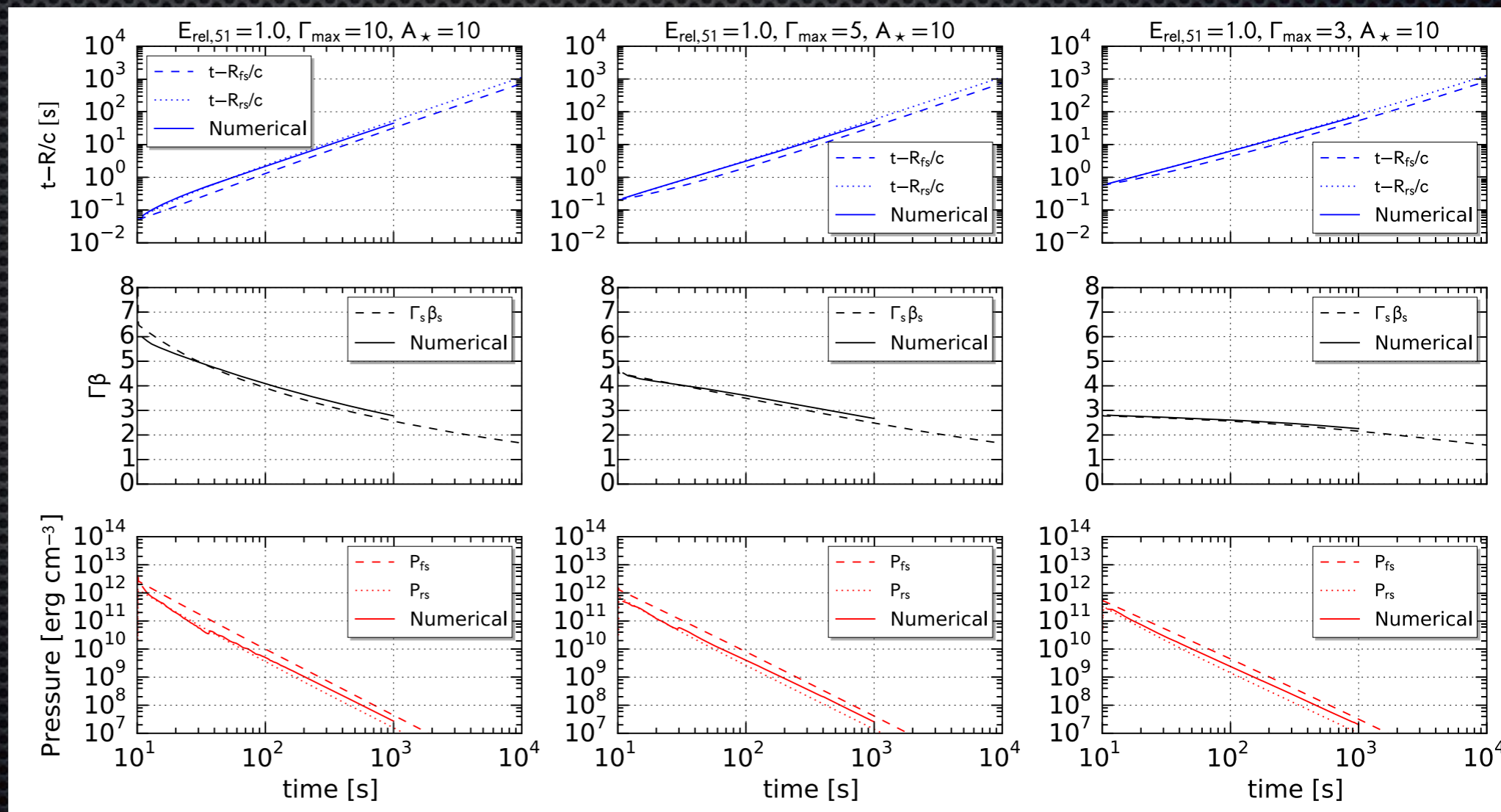


1D simulation with spherical symmetry

→ shock radii R_{fs}, R_{rs} , shell 4-velocity $\Gamma \beta$, and post-shock pressures.

Suzuki, Maeda, & Shigeyama (2017)

temporal evolution of shock radii, $\Gamma \beta$, pressure.
simulation (solid line) and semi-analytic model (dashed line)



One-zone semi-analytical model

- we approximate the shocked region as a thin shell and solve the EOM.
- shock radii R_{fs}, R_{rs} , shell mass M_s , shell momentum S_r , and so on

momentum influx from ejecta

deceleration by pressure gradient force

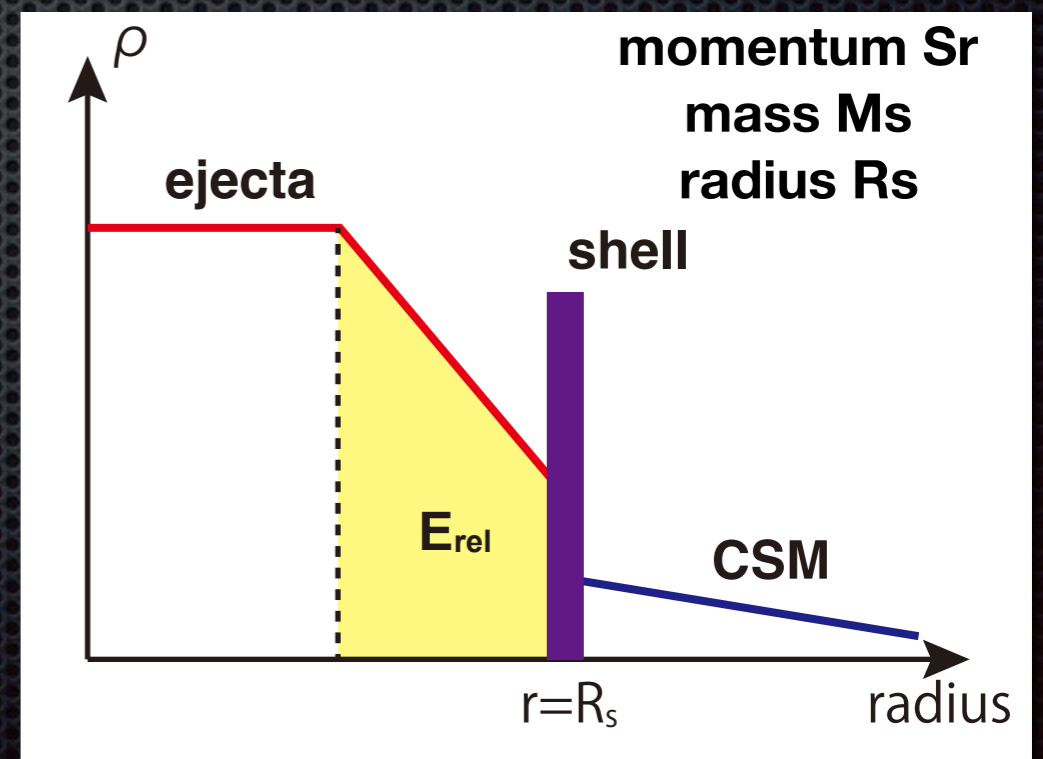
$$\frac{dS_r}{dt} + 4\pi R_{fs}^2 F_{fs} - 4\pi R_{rs}^2 F_{rs} = 4\pi R_{fs}^2 p_{rs,d} - 4\pi R_{rs}^2 p_{fs,d}$$

$$\frac{dM_s}{dt} + 4\pi R_{fs}^2 F_{m,fs} - 4\pi R_{rs}^2 F_{m,rs} = 0$$

$$\frac{dR_s}{dt} = \beta_s,$$

shell increases its mass by sweeping CSM/ejecta

forward/reverse shock velocity
determined by shock jump condition



One-zone semi-analytical model

- we approximate the shocked region as a thin shell and solve the EOM.
- shock radii R_{fs}, R_{rs} , shell mass M_s , shell momentum S_r , and so on

momentum influx from ejecta

acceleration by pressure gradient force

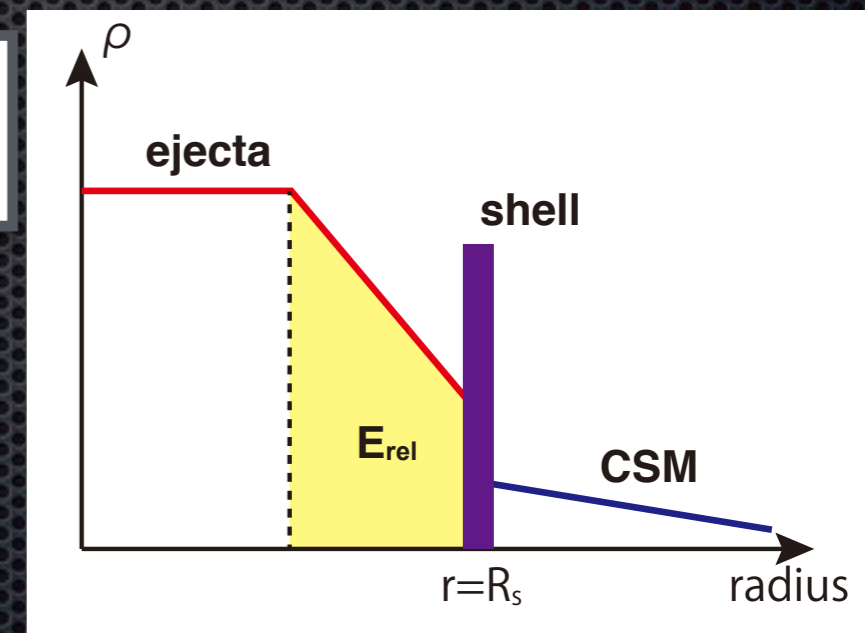
$$\frac{dS_r}{dt} + 4\pi R_{fs}^2 F_{fs} - 4\pi R_{rs}^2 F_{rs} = 4\pi R_{fs}^2 p_{rs,d} - 4\pi R_{rs}^2 p_{fs,d}$$

$$S_r = M_s \Gamma_s \beta_s \quad \Gamma_s = \sqrt{1 + \frac{S_r^2}{M_s^2}}$$

$$\beta_{sh}(\beta_u, \beta_d) = \frac{\gamma \Gamma_u \Gamma_d^2 (\beta_u - \beta_d) \beta_d - (\gamma - 1)(\Gamma_u - \Gamma_d)}{\gamma \Gamma_u \Gamma_d^2 (\beta_u - \beta_d) - (\gamma - 1)(\Gamma_u \beta_u - \Gamma_d \beta_d)}$$

$$\beta_{rs} = \beta_{sh}(\beta_{ej}, \beta_s). \quad \rho_{rs} = \rho_{ej} \frac{\Gamma_{ej}(\beta_{ej} - \beta_{rs})}{\Gamma_u(\beta_s - \beta_{rs})}, \quad p_{rs} = \frac{\rho_{ej} \Gamma_{ej}^2 (\beta_{ej} - \beta_{rs})(\beta_{ej} - \beta_s)}{1 - \beta_s \beta_{rs}}$$

$$F_{rs} = \rho_{ej} \Gamma_{ej}^2 \beta_{ej} (\beta_{ej} - \beta_{rs}),$$

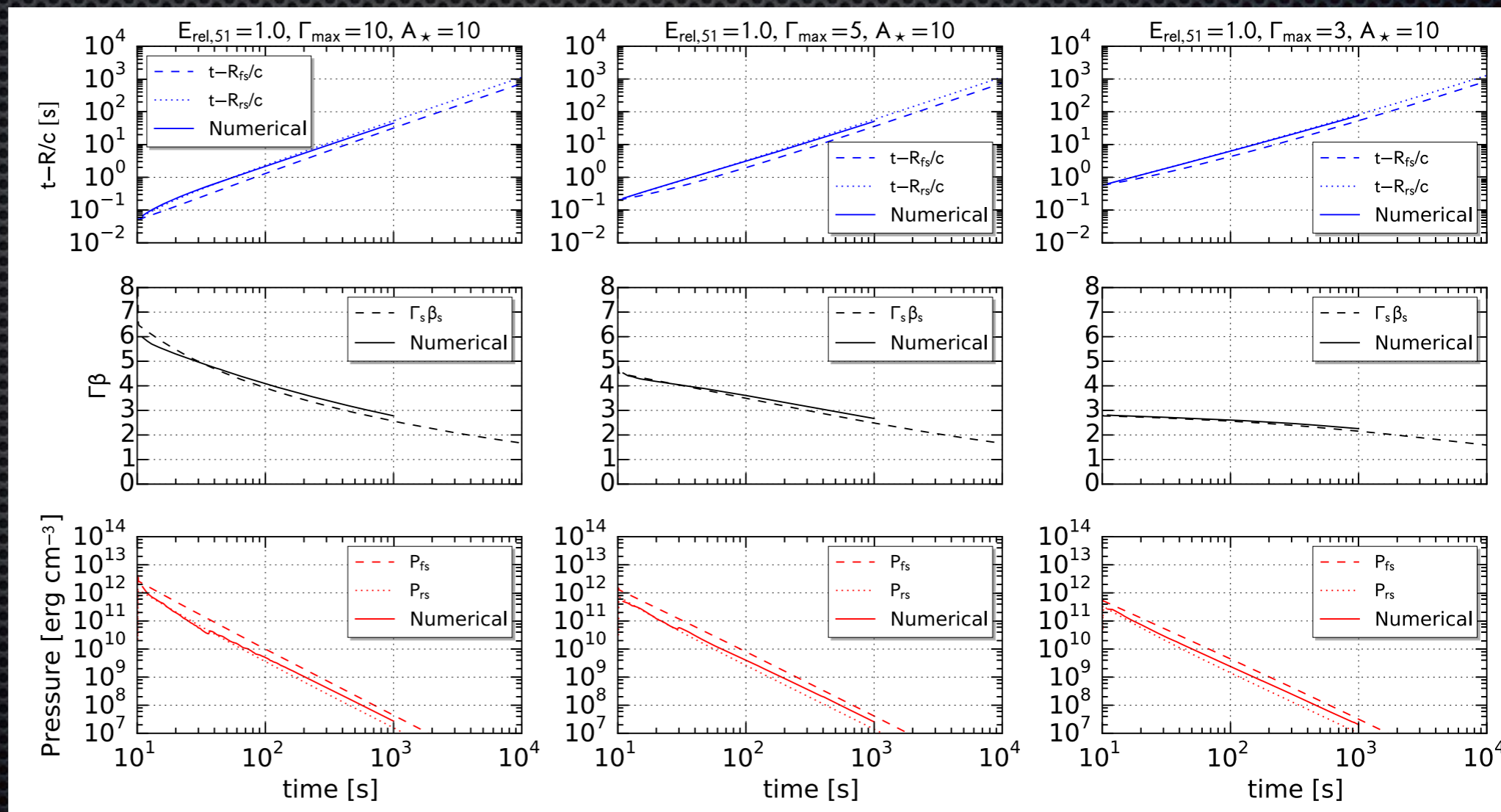


One-zone semi-analytical model

- we approximate the shocked region as a thin shell and solve the EOM.
- shock radii R_{fs}, R_{rs} , shell mass M_s , shell momentum S_r , and so on
- consistent with numerical simulations

Suzuki, Maeda, & Shigeyama (2017)

temporal evolution of shock radii, Γ , β , pressure.
simulation (solid line) and semi-analytic model (dashed line)



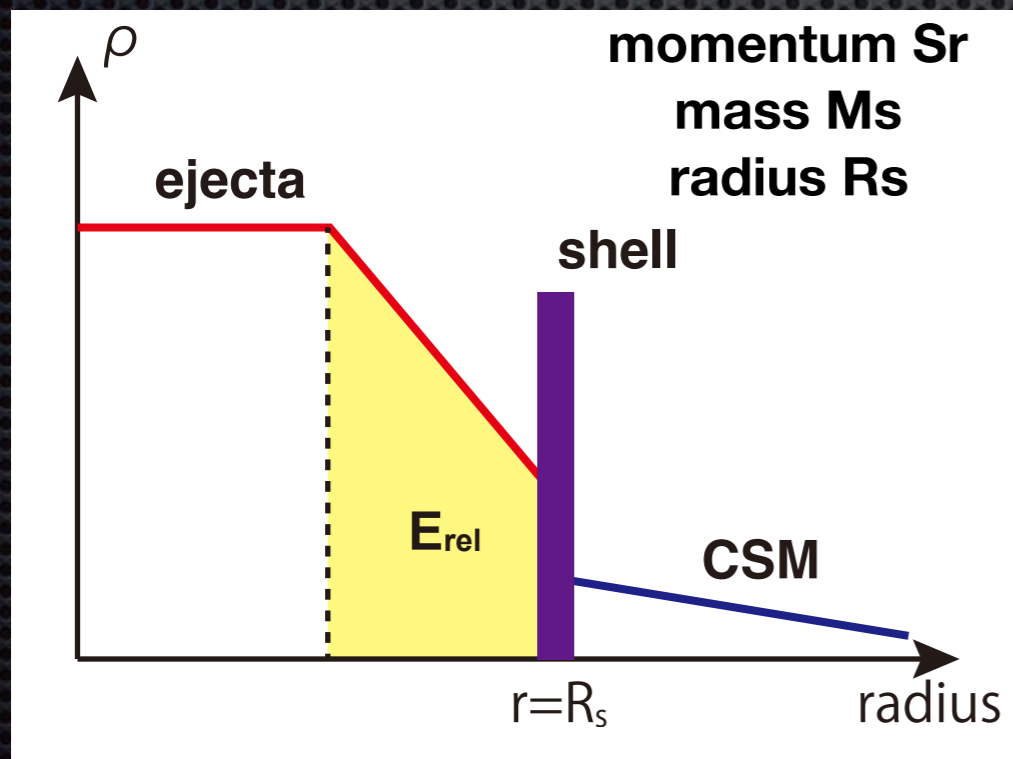
Emission model

Suzuki, Maeda, & Shigeyama (2017, 2018 in prep)

- temporal evolution of the internal energy of the shell is solved.
- the internal energy is lost by radiative diffusion and adiabatic cooling.
- radiative loss rate corresponds to the luminosity of the diffusive emission

adiabatic loss radiative loss

$$\frac{dE_{s,\text{rad}}}{dt} = \dot{E}_{\text{fs}} + \dot{E}_{\text{rs}} - \frac{E_{s,\text{rad}}}{3V} \frac{dV}{dt} - \dot{E}_{\text{diff}},$$



$$\dot{E}_{\text{diff}} = 4\pi R_s^2 u_{s,\text{rad}} v_{\text{diff}}$$

$$v_{\text{diff}} = \frac{c(1 - \beta_s^2)}{(3 + \beta_s^2)\tau_s + 2\beta_s},$$

- diffusion approximation: optical depth τ ($\kappa = 0.2 \text{ cm}^2/\text{g}$), velocity β_s , and internal energy density u_{rad}

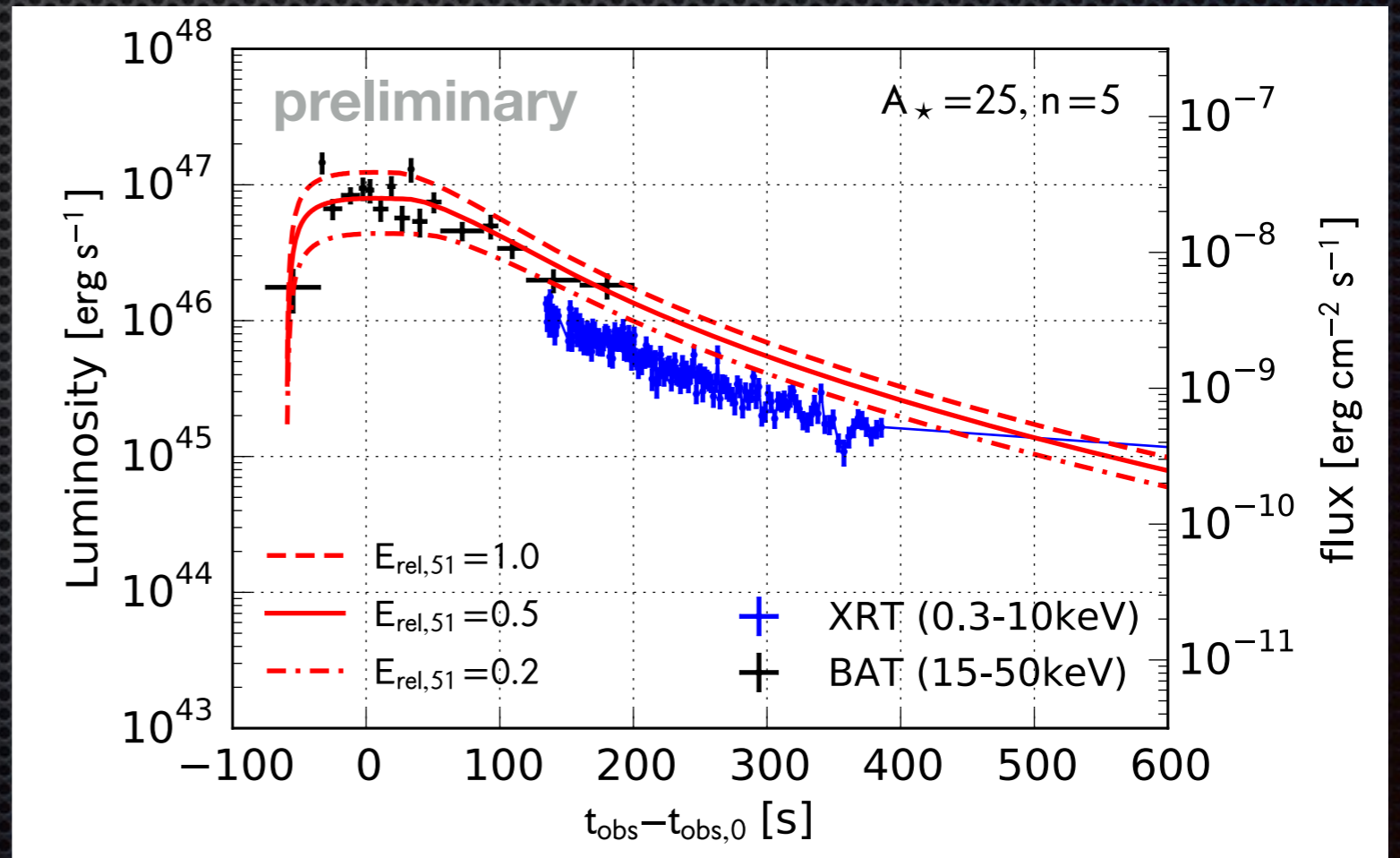
$$L_{\text{diff}}(t_{\text{obs}}) = c \int \frac{\dot{E}_{\text{diff}}(t)}{R_s(t)\Gamma_s^3 [1 - \mu\beta_s(t)]^3} dt,$$

- Introduction
- Ejecta-CSM interaction
- Light curve fitting for GRB171205A
- Conclusion

Bolometric LC for prompt emission

- ➔ fiducial model: $E_{\text{rel},51}=0.5, A_{\star}=25, n=5$ ($dM/dt=2.5 \times 10^{-4} M_{\odot}/\text{yr}$ for $v_w=10^3 \text{ km/s}$)
- ➔ theoretical emission model is consistent with observed prompt gamma-ray and X-ray light curves
- ➔ note: theoretical model produce bolometric light curves
- ➔ spectral evolution is the next step

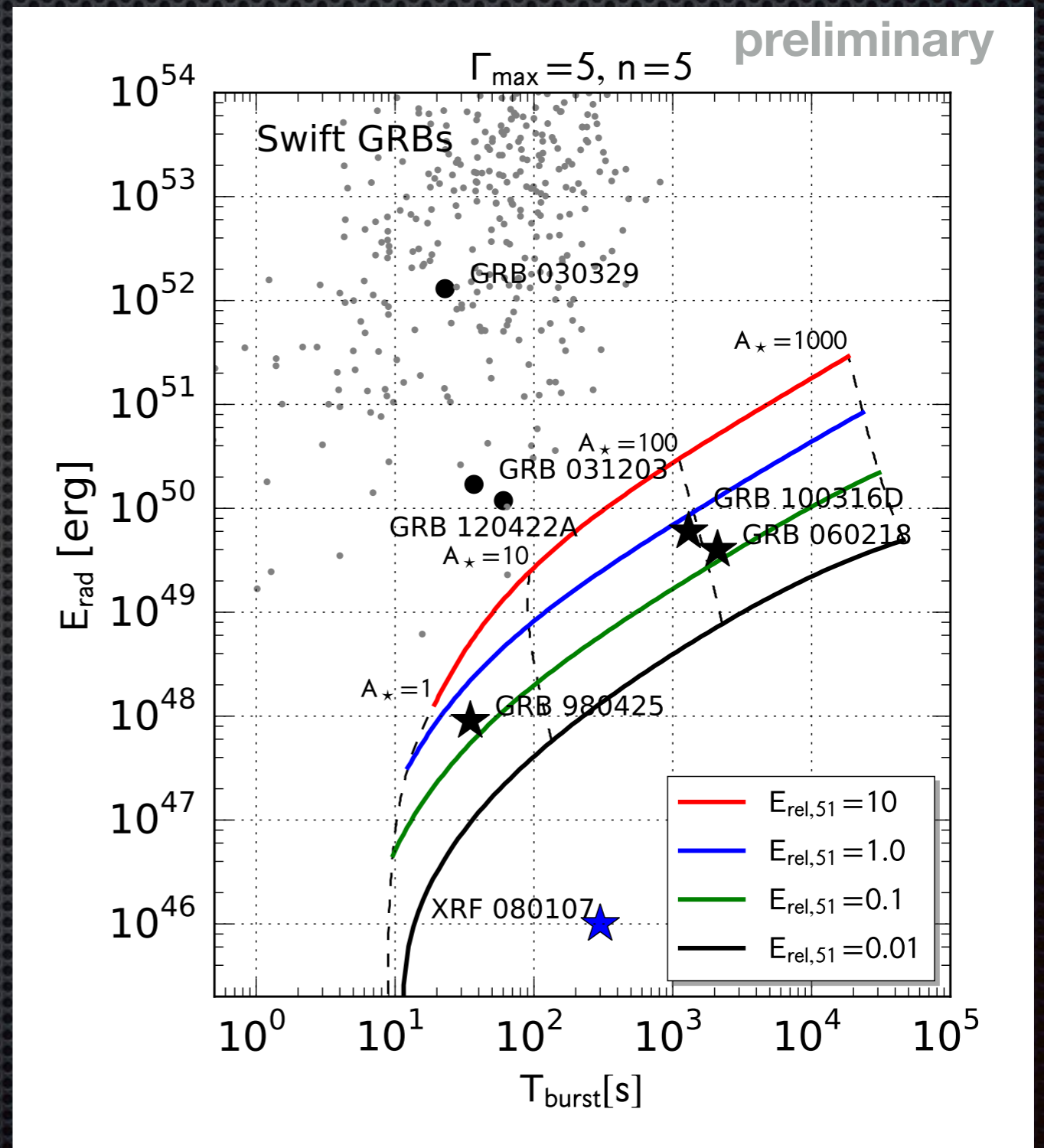
Suzuki, Maeda, & Shigeyama (2018, in prep)



E_{rad} VS T_{burst}

- ➔ $E_{\text{rad}}-T_{\text{burst}}$ diagram
- ➔ longer bursts show larger radiated energies
- ➔ in ejecta-CSM interaction model, this trend can be explained by increasing CSM density (or mass)
- ➔ GRB 171205A is consistent with the trend.
- ➔ GRB171205A: $E_{\text{rel}} \sim 10^{51}$ [erg], $A_{\star} \sim$ several 10

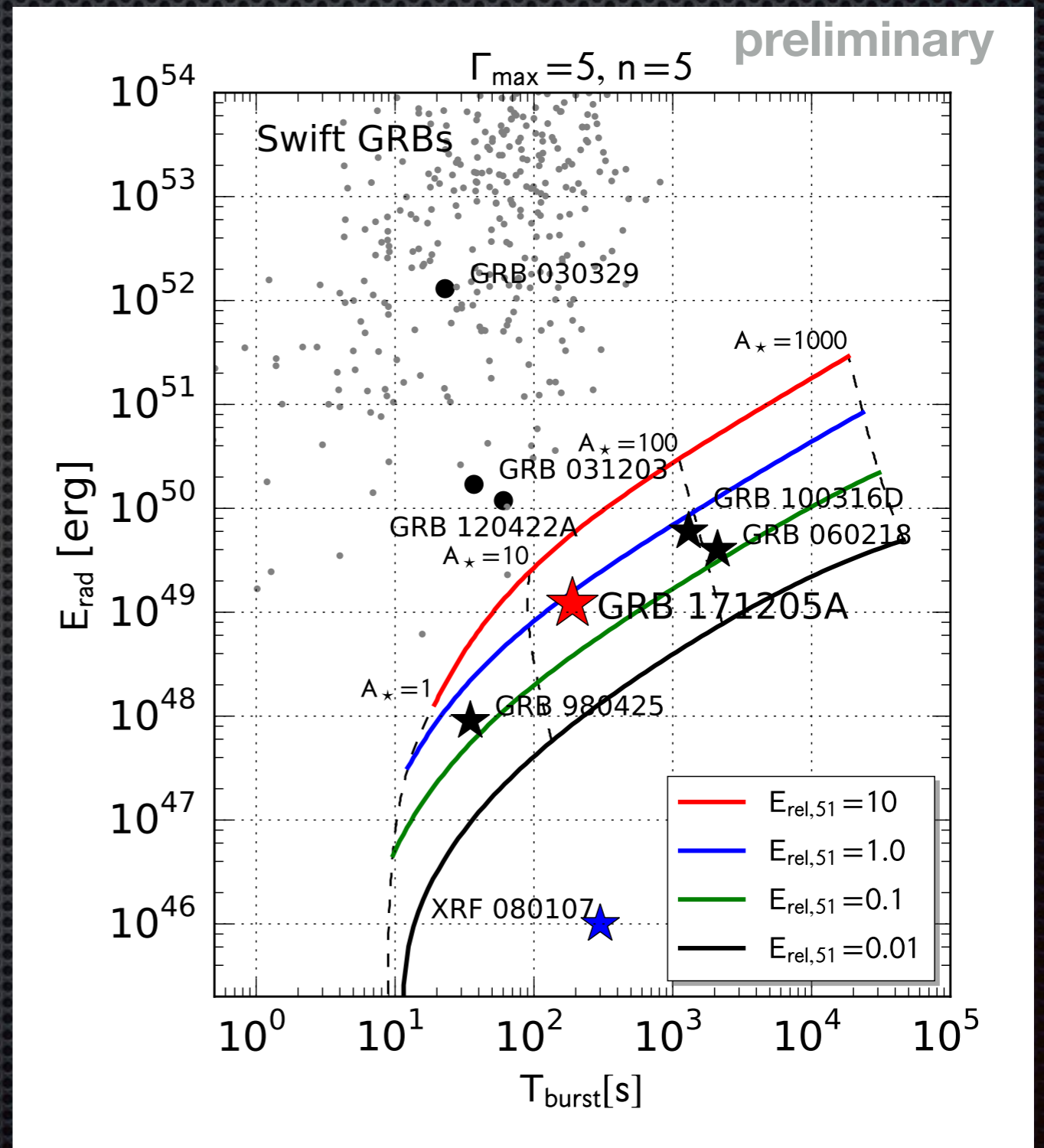
Suzuki, Maeda, & Shigeyama (2018, in prep)



E_{rad} VS T_{burst}

- ➔ $E_{\text{rad}}-T_{\text{burst}}$ diagram
- ➔ longer bursts show larger radiated energies
- ➔ in ejecta-CSM interaction model, this trend can be explained by increasing CSM density (or mass)
- ➔ GRB 171205A is consistent with the trend.
- ➔ GRB171205A: $E_{\text{rel}} \sim 10^{51}$ [erg], $A_{\star} \sim$ several 10

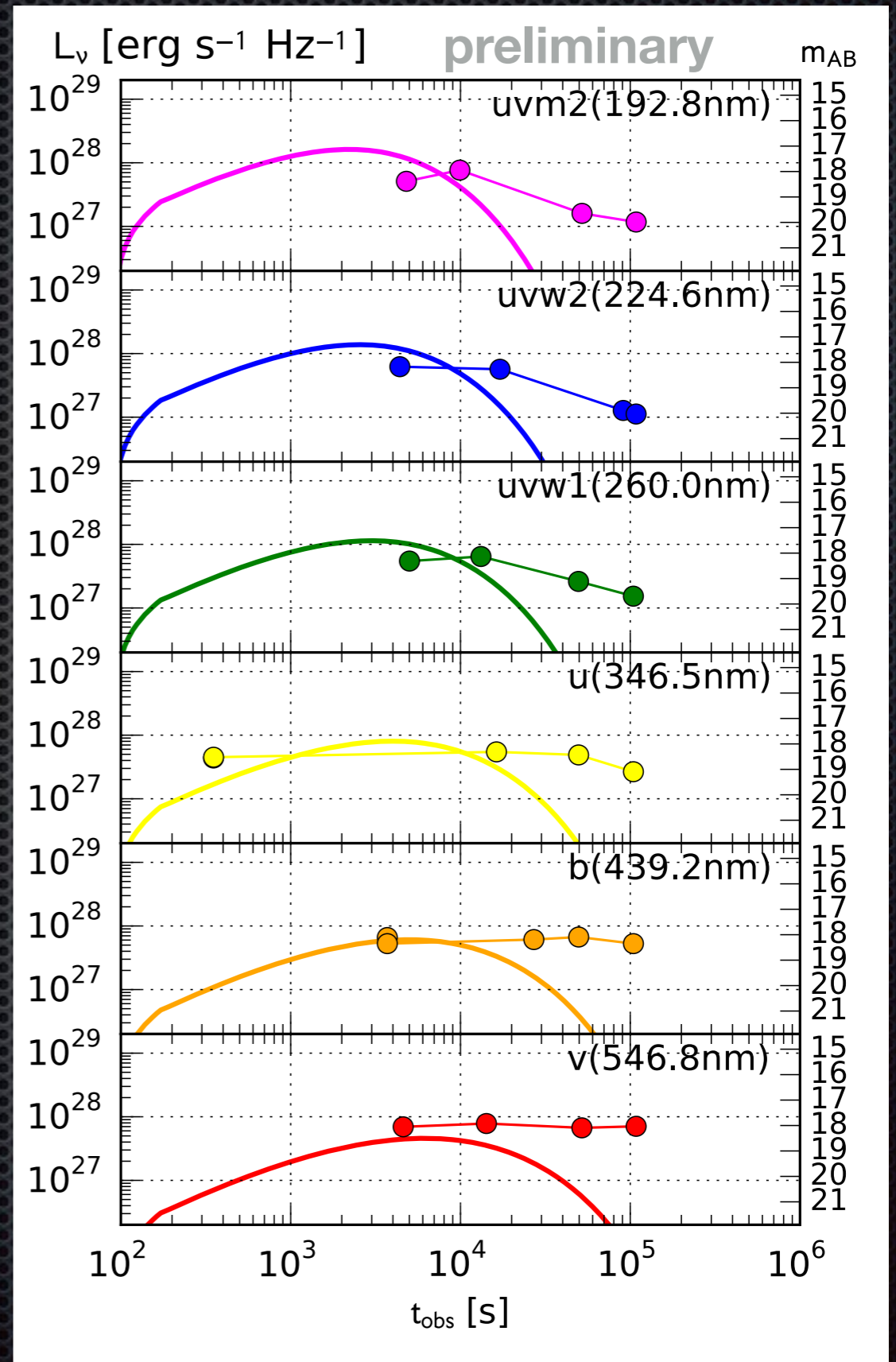
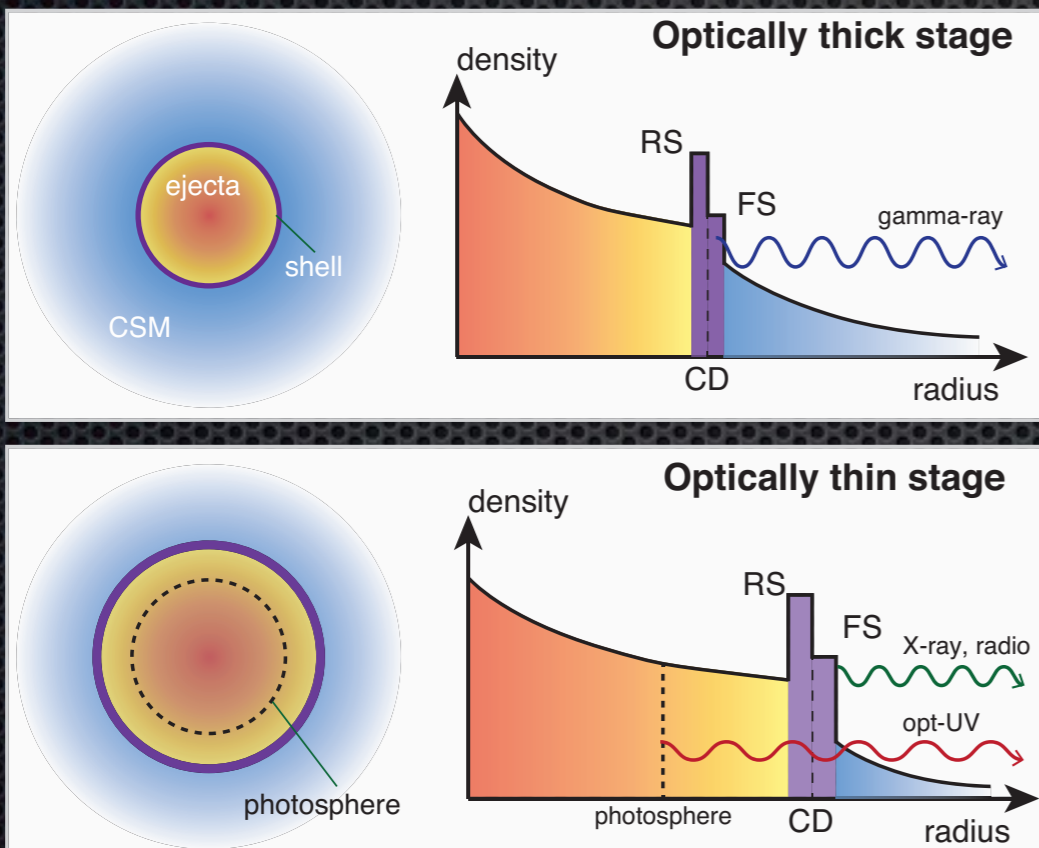
Suzuki, Maeda, & Shigeyama (2018, in prep)



Optical-UV emission

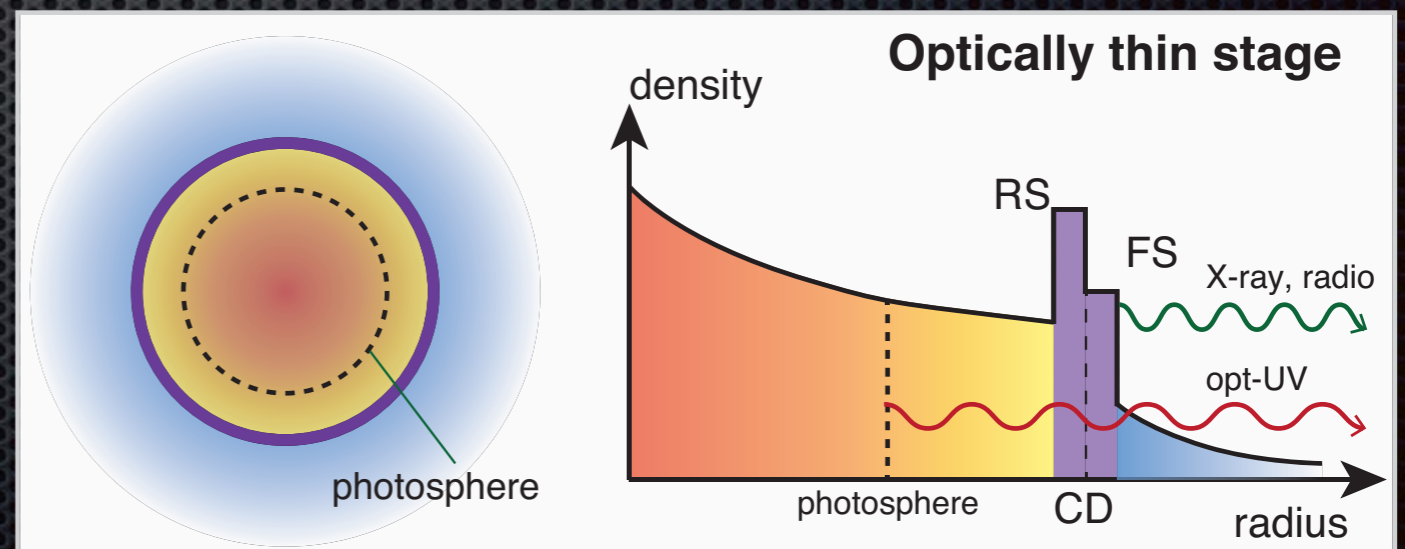
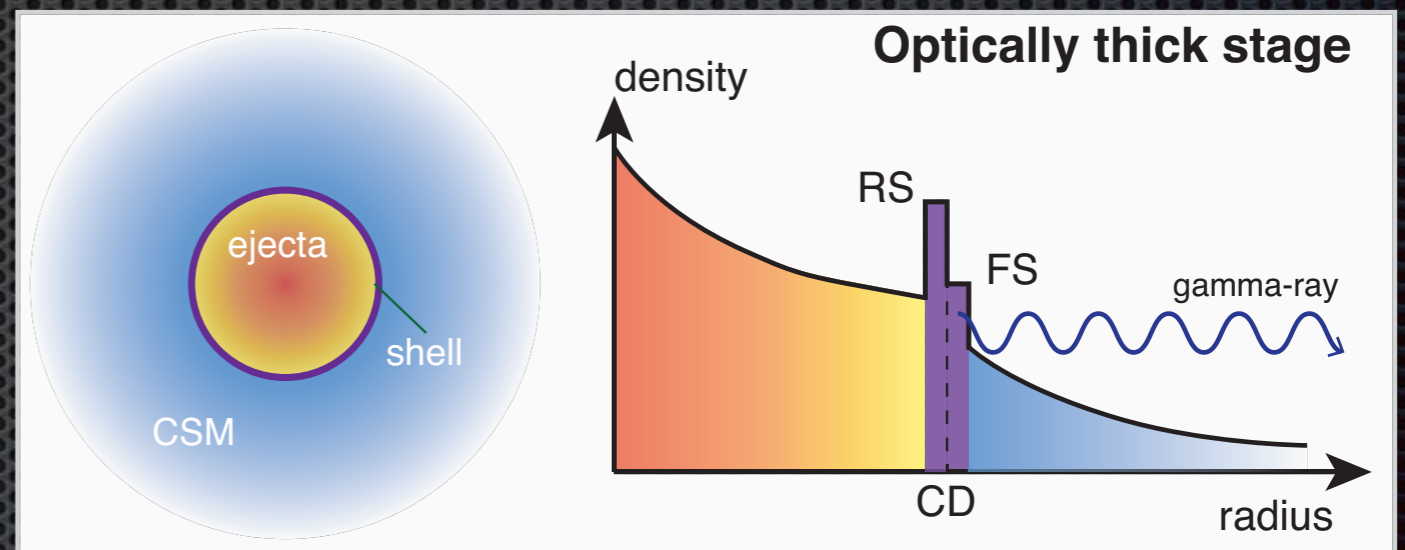
- Swift UVOT observations
- a parameter $f_{th}=0.03$: radiation energy to kinetic energy ratio of the ejecta at $t=t_0$

Suzuki, Maeda, & Shigeyama (2018, in prep)



Multi-wavelength LC modeling

- prompt emission of GRB 171205A could be explained by mildly relativistic SN ejecta interacting with a dense CSM.
- What about other EM signals?
- opt-UV observations by UVOT
- radio, X-ray non-thermal emission



Non-thermal X-ray and radio emission

- electron distribution in momentum space
- parameters: ρ , ϵ_e , ϵ_B
- synchrotron, inverse Compton, and adiabatic cooling

Suzuki, Maeda, & Shigeyama (2018, in prep)

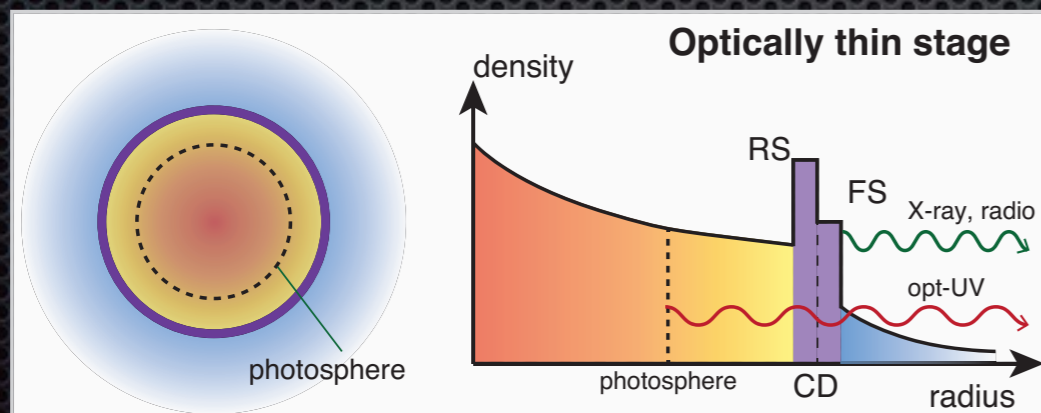
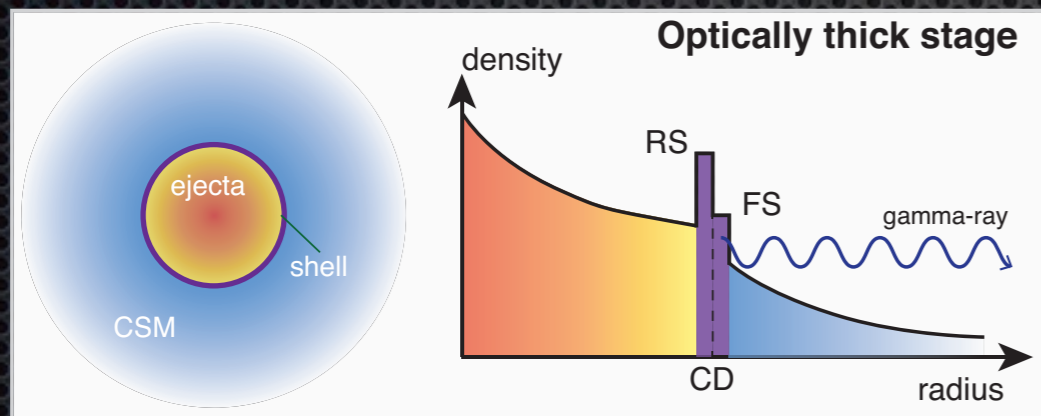
$$\frac{\partial}{\partial t} \left(\frac{dN}{dp_e} \right) = \frac{\partial}{\partial p_e} \left[(\dot{p}_{\text{syn}} + \dot{p}_{\text{ic}} + \dot{p}_{\text{ad}}) \frac{dN}{dp_e} \right] + \left(\frac{d\dot{N}}{dp_e} \right)_{\text{in}}$$

$$\left(\frac{d\dot{N}}{dp_e} \right)_{\text{in}} \propto \begin{cases} p_e^{-P} & \text{for } p_{\text{in}} \leq p_e \leq p_{\text{max}} \\ 0 & \text{otherwise} \end{cases}$$

$$\dot{p}_{\text{syn}} = \frac{4\sigma_T u_B}{3m_e^2 c^2} p_e \sqrt{m_e^2 c^2 + p_e^2},$$

$$\dot{p}_{\text{ic}} = \frac{4\sigma_T u_{\text{rad}}}{3m_e^2 c^2} p_e \sqrt{m_e^2 c^2 + p_e^2},$$

$$\dot{p}_{\text{ad}} = \frac{p_e}{3V} \frac{dV}{dt}.$$

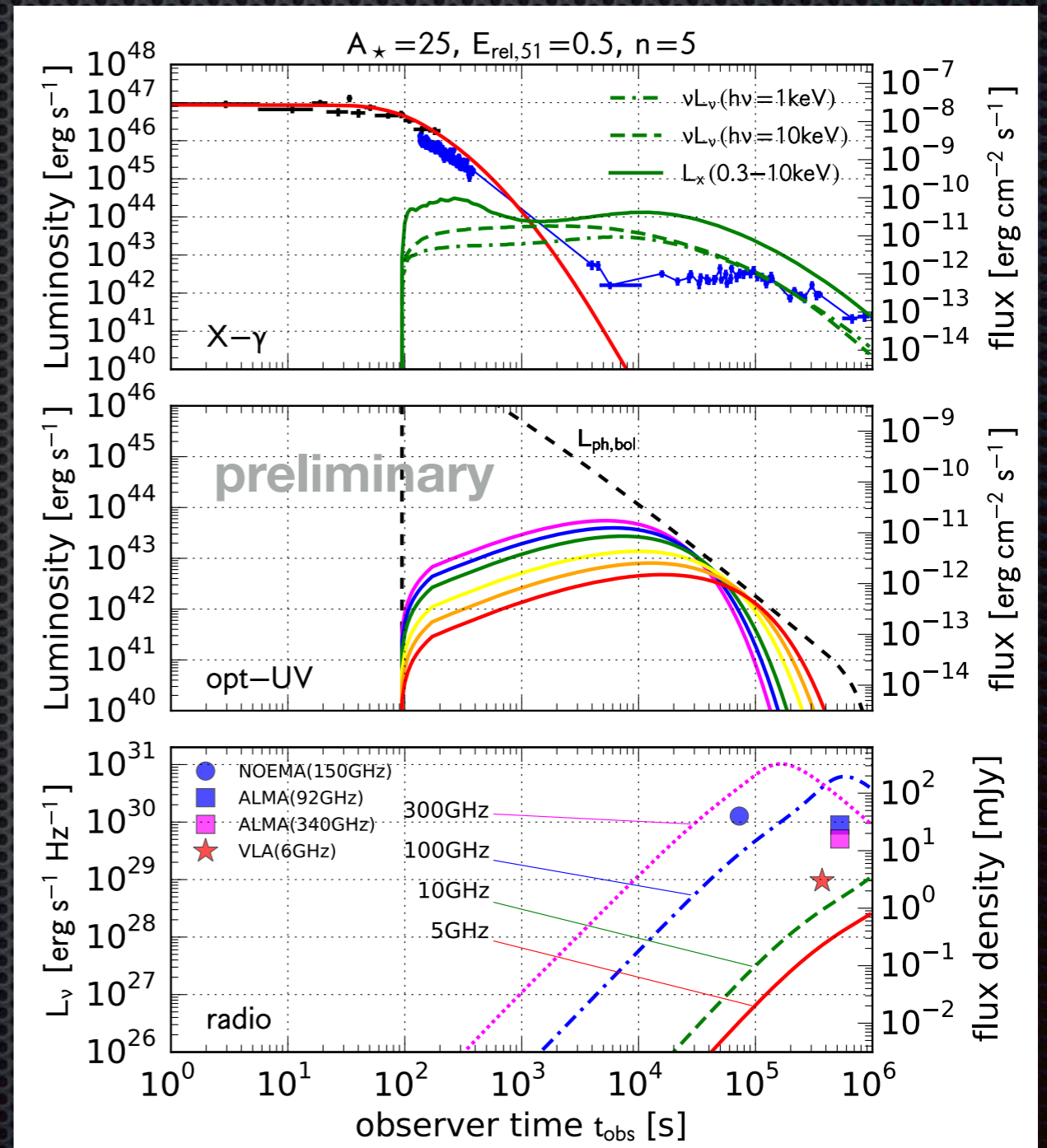
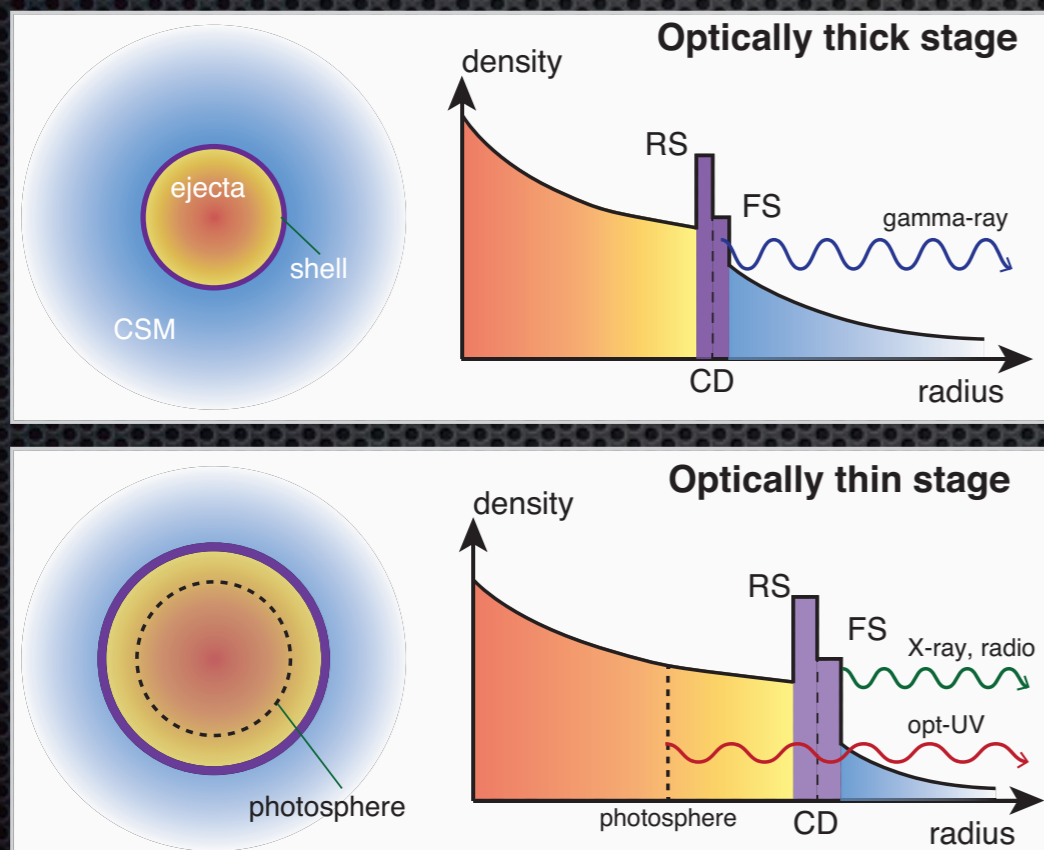


→ u_{rad} : thermal photons+ synchrotron photons

Non-thermal X-ray and radio emission

- ➔ $p=3.0, \varepsilon_e=0.08, \varepsilon_B=3 \times 10^{-3}$
- ➔ Swift XRT observations + radio (NOEMA, ALMA, VLA)
- ➔ too bright inverse Compton X-ray emission...
- ➔ too high A_\star beyond $r \sim 3 \times 10^{13} \text{cm}$?

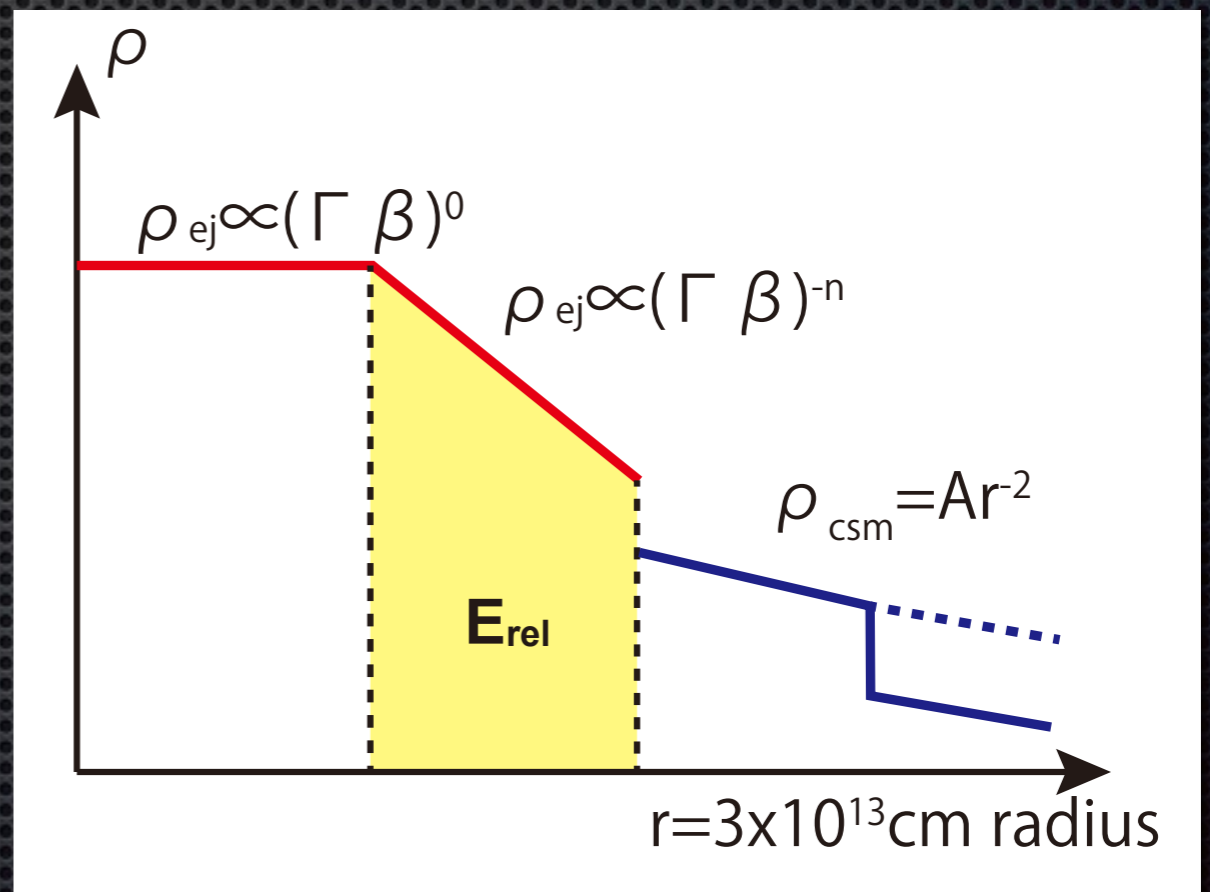
Suzuki, Maeda, & Shigeyama (2018, in prep)



Non-thermal X-ray and radio emission

- $p=3.0, \epsilon_e=0.08, \epsilon_B=3 \times 10^{-3}$
- Swift XRT observations + radio (NOEMA, ALMA, VLA)
- too bright inverse Compton X-ray emission...
- too high A_\star beyond $r \sim 3 \times 10^{13} \text{cm}$?

Suzuki, Maeda, & Shigeyama (2018, in prep)

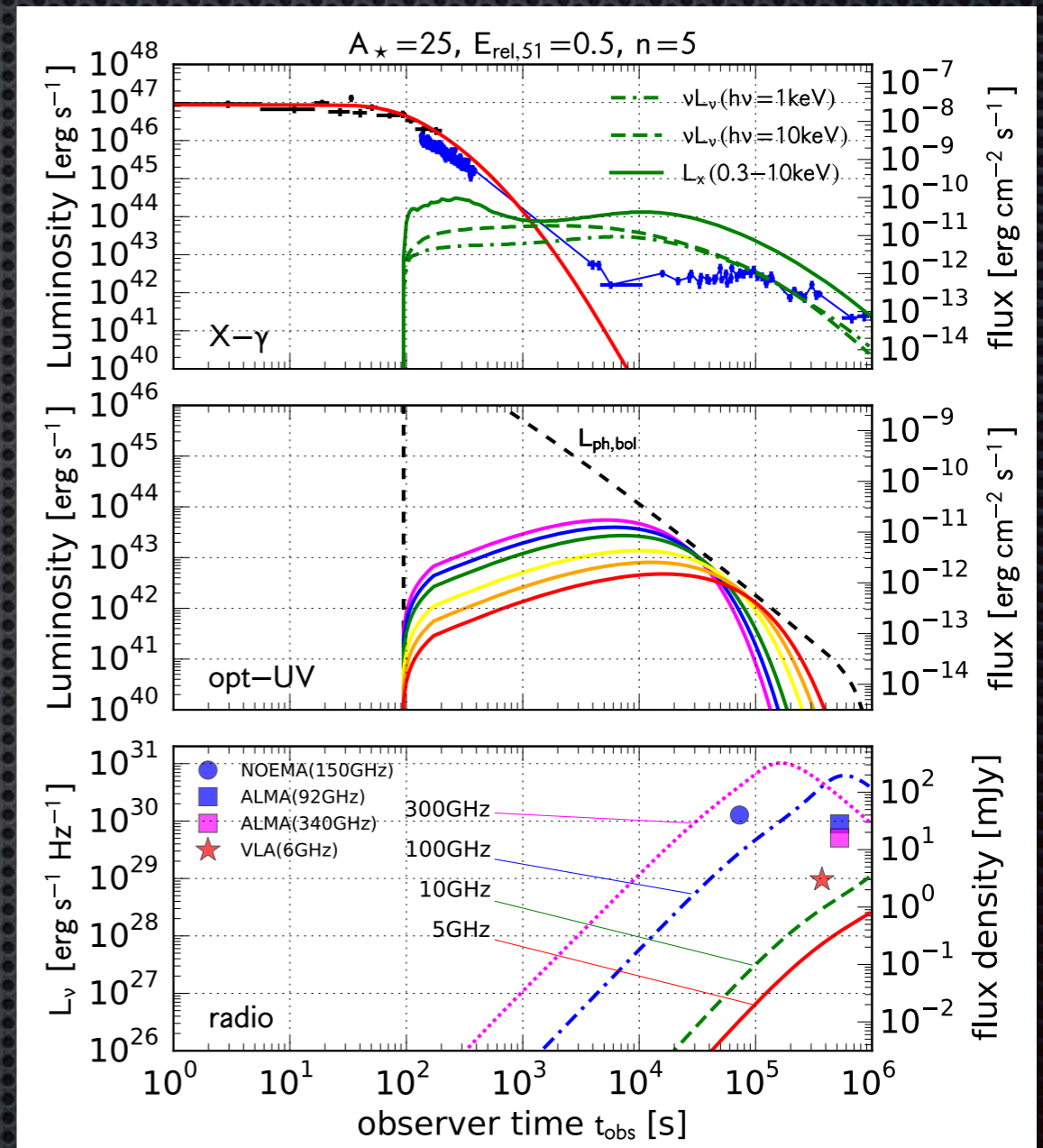
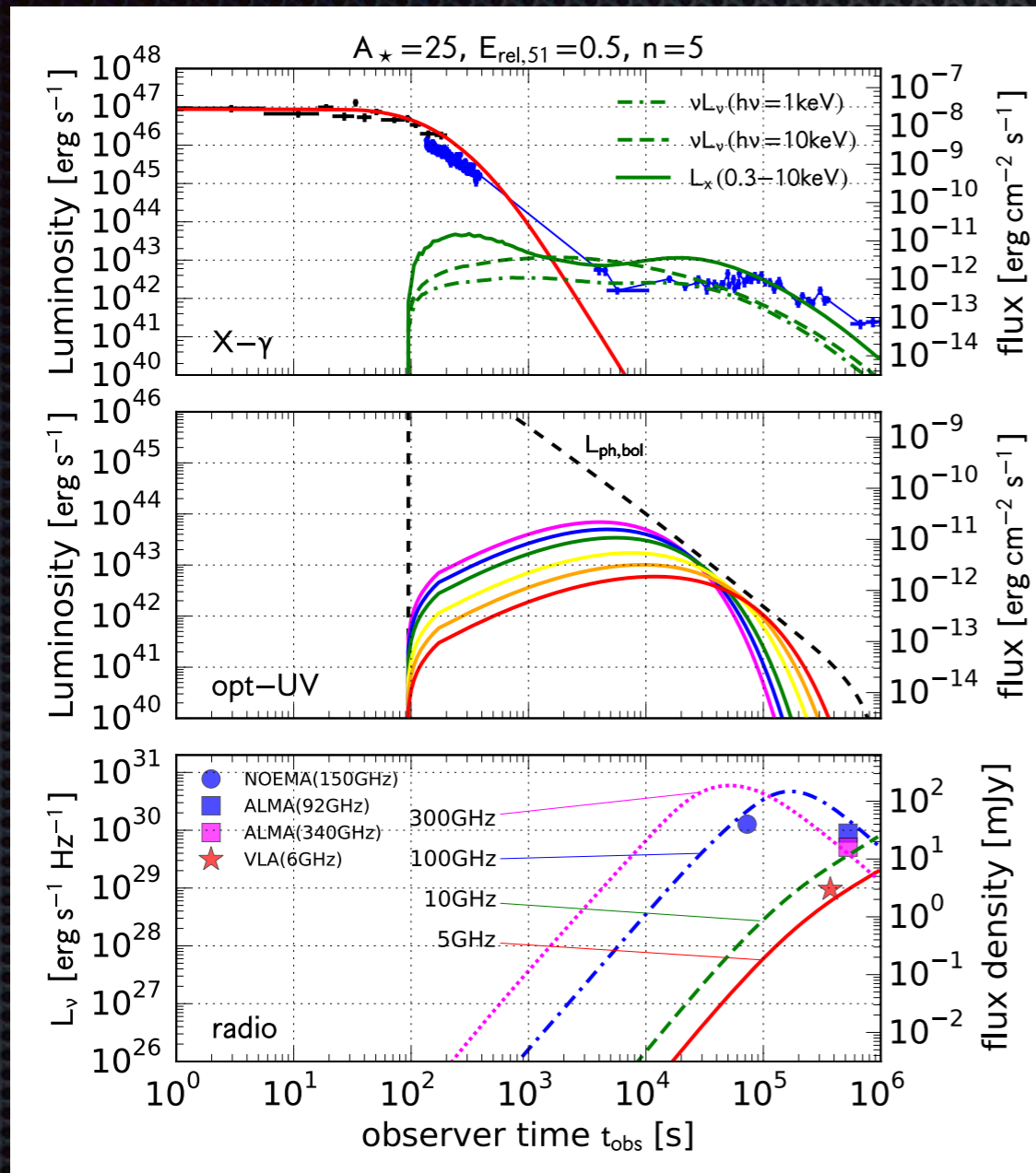


- reduced CSM density at $r > 3 \times 10^{13} \text{cm}$: $A_\star = 25 \rightarrow 0.5$

Non-thermal X-ray and radio emission

Suzuki, Maeda, & Shigeyama (2018, in prep)

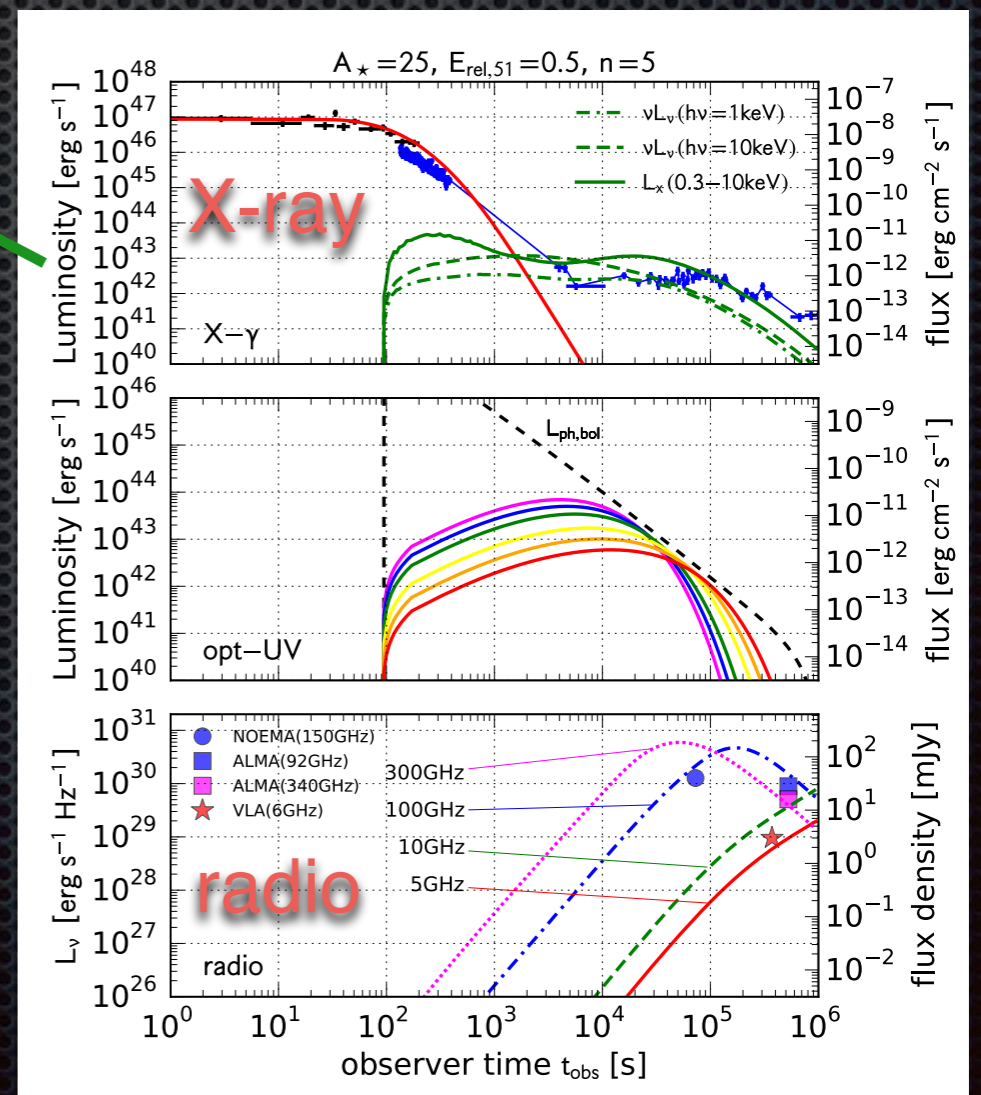
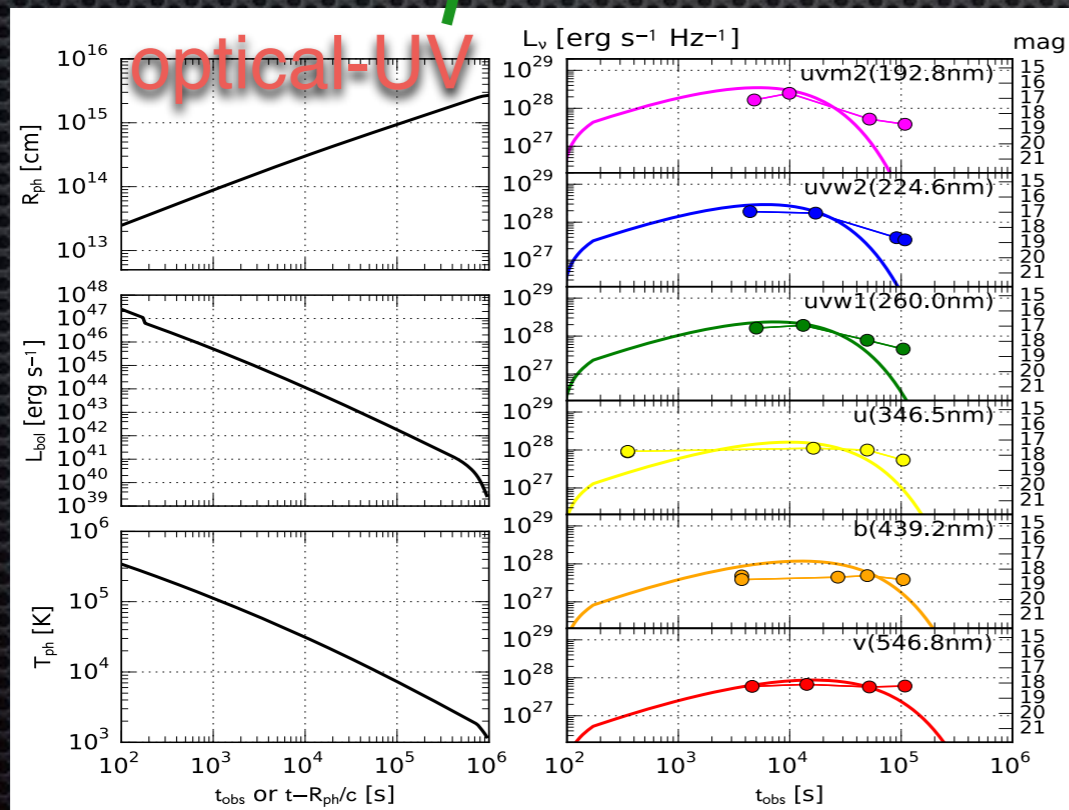
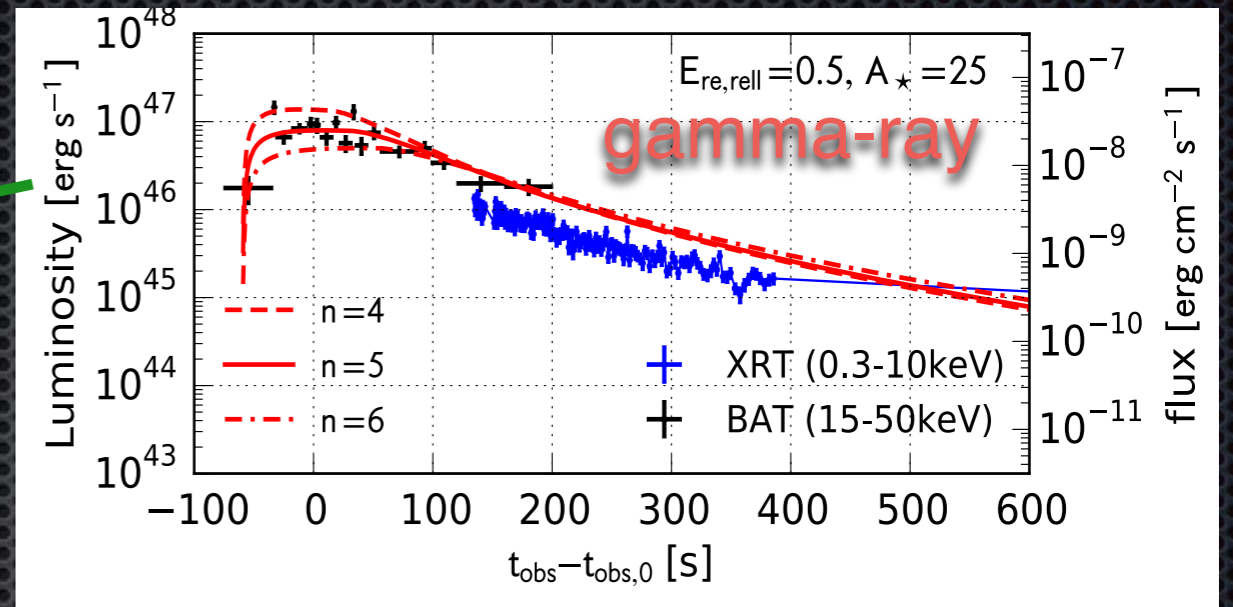
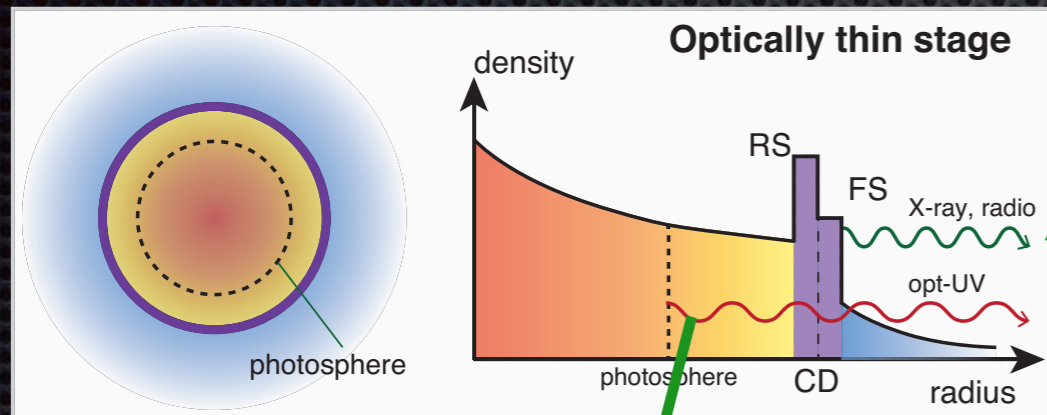
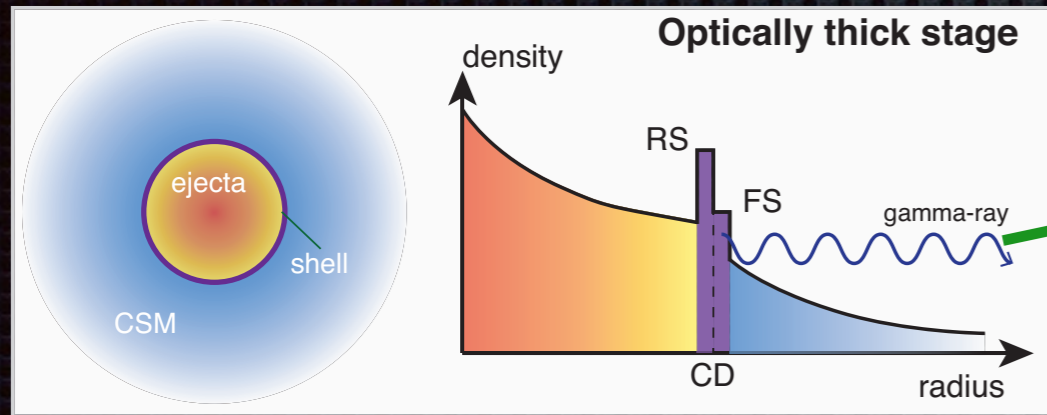
reduced A_{\star} model



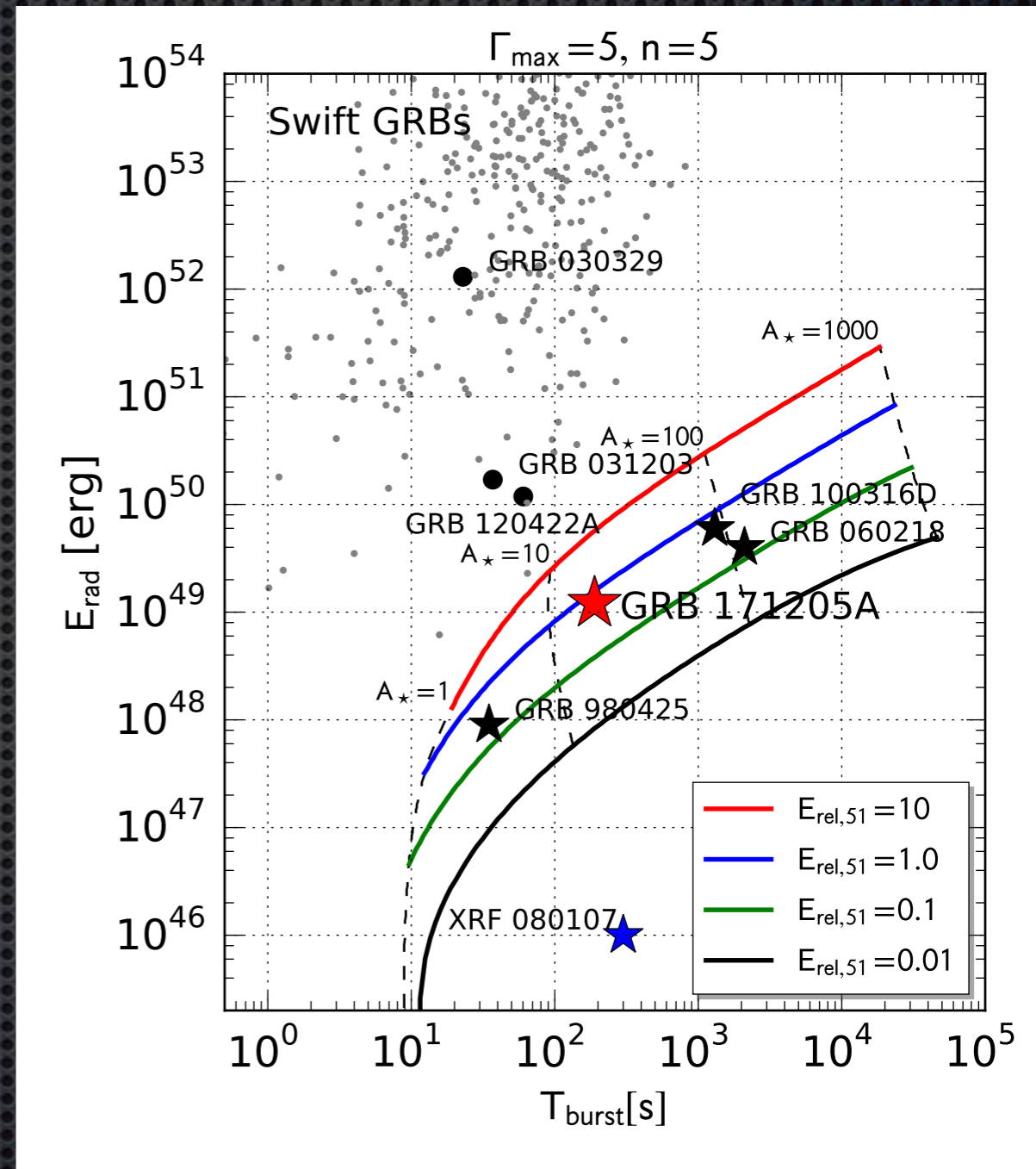
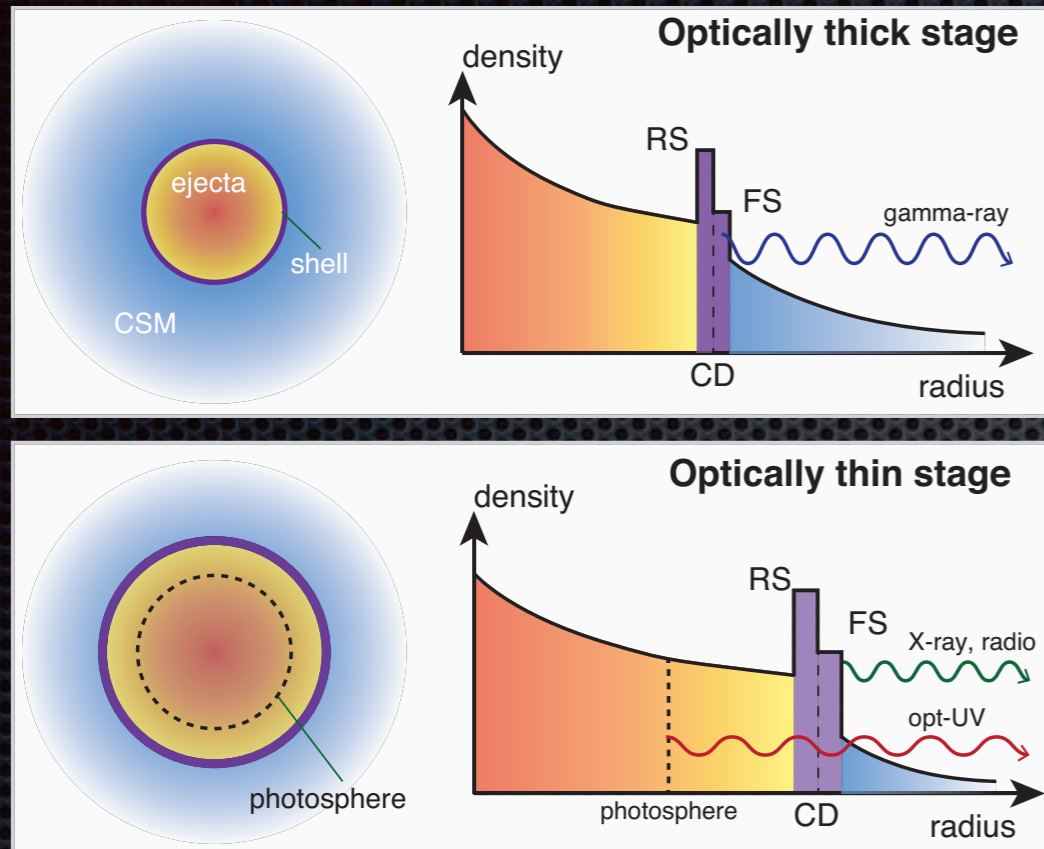
→ reduced CSM density at $r > 3 \times 10^{13} \text{cm}$: $A_{\star} = 25 \rightarrow 0.5$

- Introduction
- Ejecta-CSM interaction
- Light curve fitting for GRB171205A
- Conclusion

Discussion and Conclusions



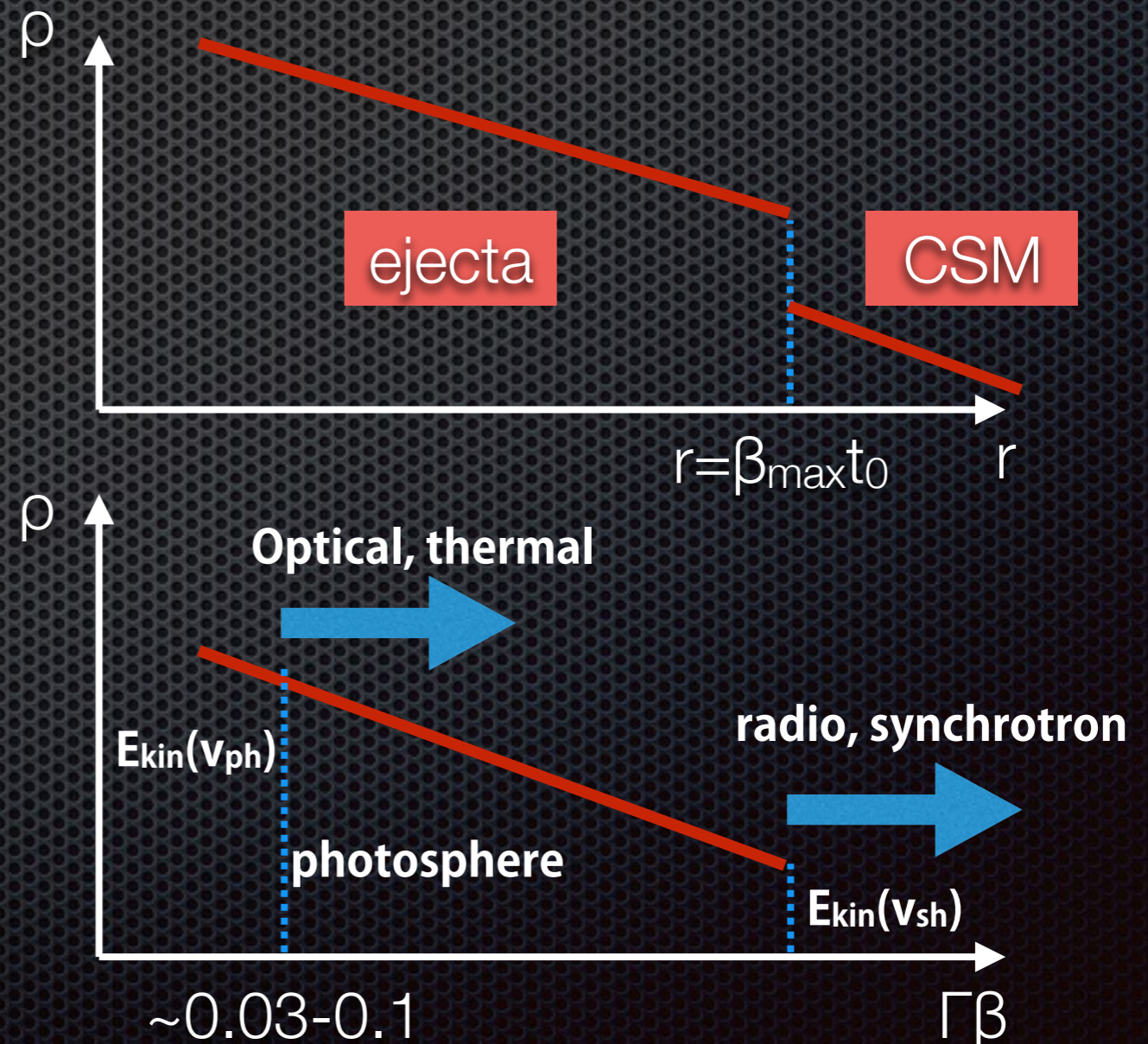
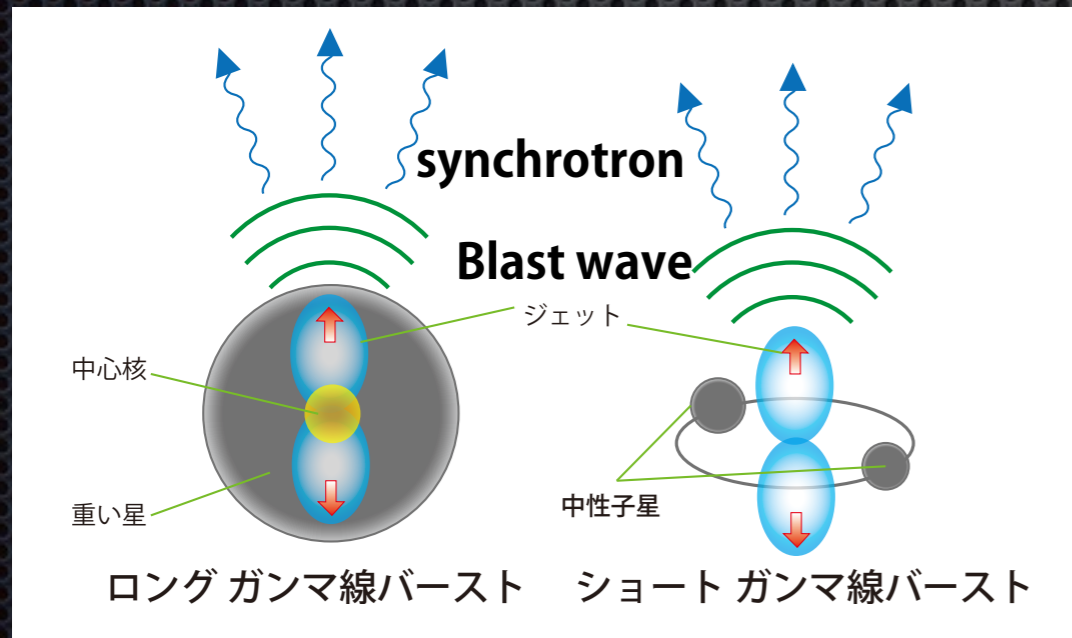
Discussion and Conclusions



- ➔ multi-wavelength emission model based on relativistic ejecta-CSM interaction scenario
- ➔ what is the origin of relativistic ejecta? failed jet? cocoon?
- ➔ CSM structure?
- ➔ gamma-ray spectrum?

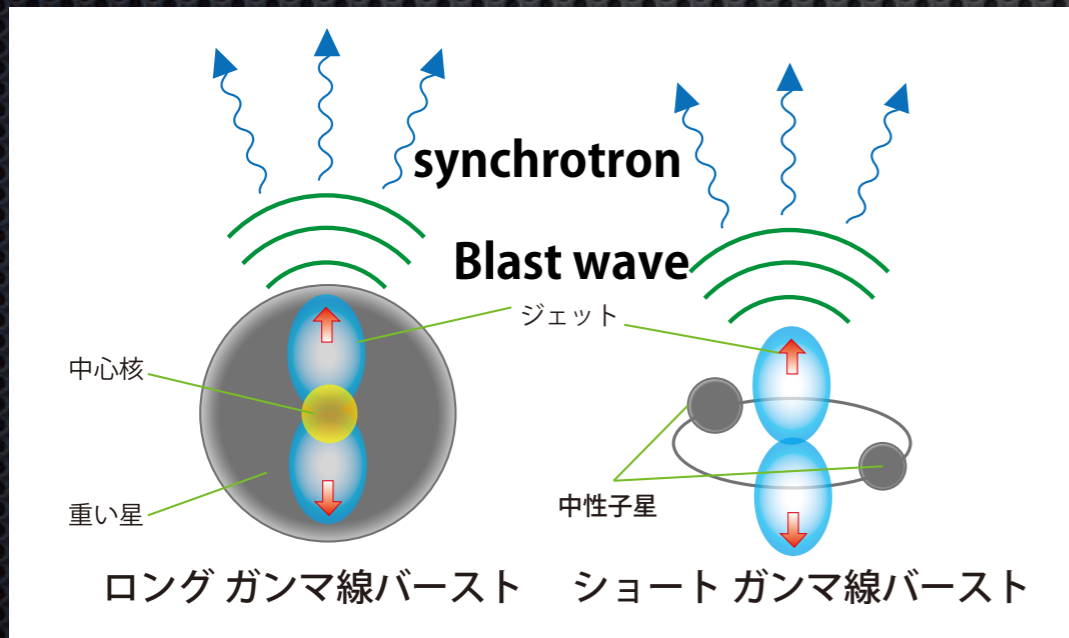
Radio observations of synchrotron emitting blast wave

- radio loud & radio quiet populations correspond normal GRBs and SNe
- 4-velocity of blast wave, $\Gamma \beta \sim 1-2$ for sub-energetic GRBs
- radio observations imply steeper kinetic energy distributions than normal GRBs

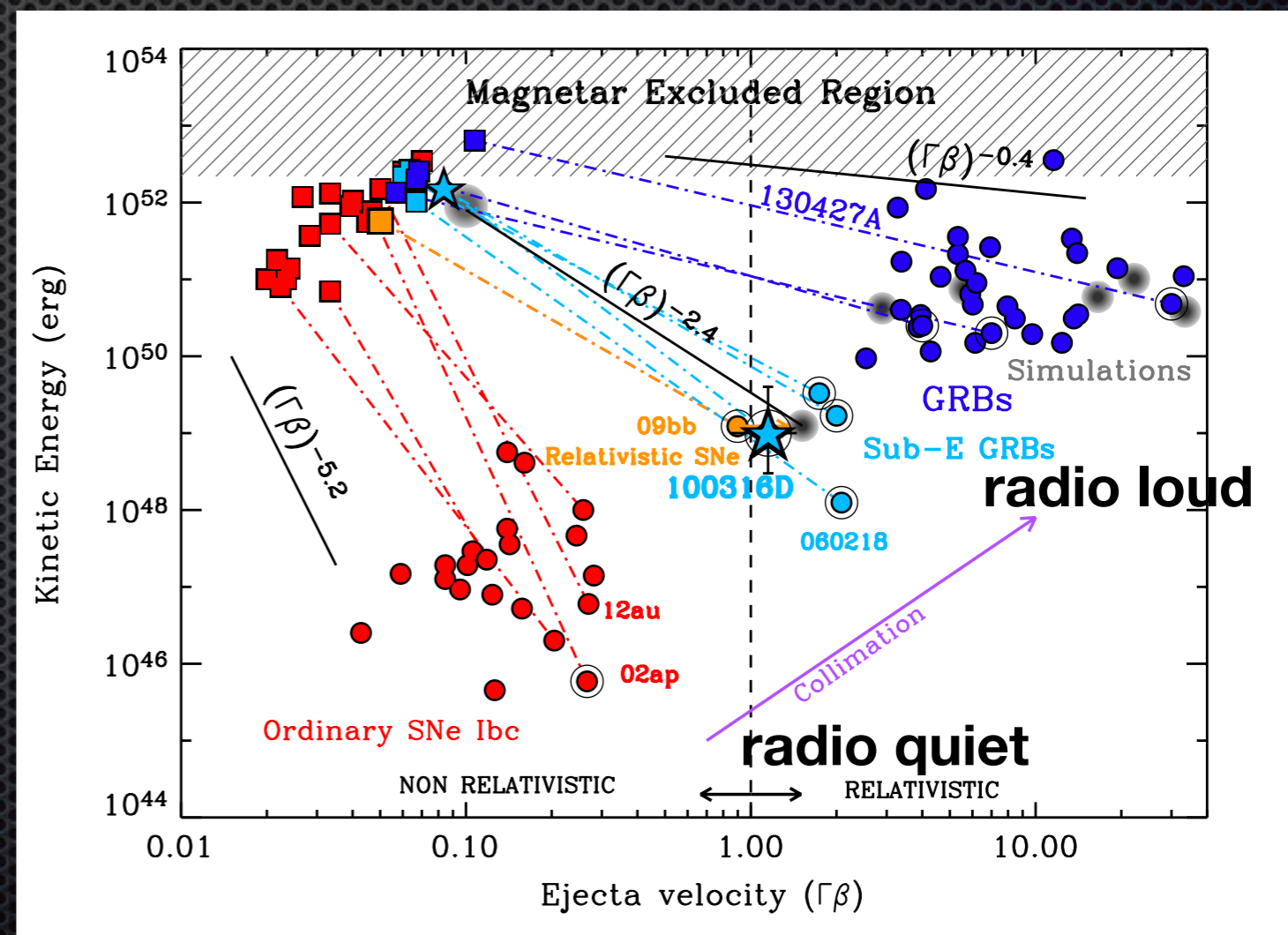


Radio observations of synchrotron emitting blast wave

- radio loud & radio quiet populations correspond normal GRBs and SNe
- 4-velocity of blast wave, $\Gamma \beta \sim 1-2$ for sub-energetic GRBs
- radio observations imply steeper kinetic energy distributions than normal GRBs

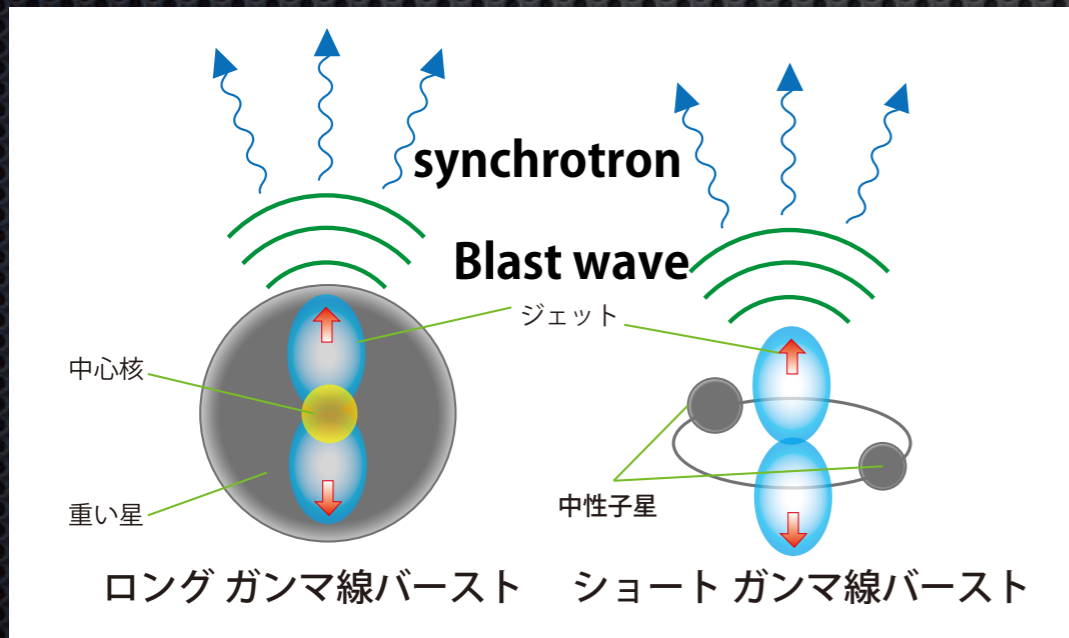


Margutti+ (2013)



Radio observations of synchrotron emitting blast wave

- radio loud & radio quiet populations correspond normal GRBs and SNe
- 4-velocity of blast wave, $\Gamma \beta \sim 1-2$ for sub-energetic GRBs
- radio observations imply steeper kinetic energy distributions than normal GRBs



Margutti+ (2013)

